Chapter 5:

Genotypic and phenotypic study of virulence factors in *K. pneumoniae*

5.1 Introduction

Klebsiella pneumoniae, a member of the *Enterobacteriaceae* family, is an infectious agent associated with many illnesses in both community and healthcare environments. These infections include pneumonia, bacteremia, urinary tract infections, and pyogenic liver abscesses (Brhelova et al., 2017). The virulence factors of *K. pneumoniae* that have been thoroughly investigated include the capsule, lipopolysaccharides (LPS), and siderophores. These variables play a critical role in the context of adhesion, colonization, invasion, and the subsequent spread of infection (Paczosa & Mecsas, 2016). Recent discoveries of virulence factors include many components, such as outer membrane proteins, efflux pumps, iron transport systems, porins, and genes related to allantoin metabolism (Remya et al., 2019). There are two major surface antigen sugars produced by *K. pneumoniae* are lipopolysaccharide and capsule polysaccharide (CPS). The capsule is the outermost component and a virulence feature of *K. pneumoniae* and other infectious bacteria. It is recognized as an effective barrier that helps evade the host's innate immune response (Comstock & Kasper, 2006; Rendueles, 2020). Each kind has distinct structural variations that occur in the repetitive polysaccharide block of capsular polysaccharide (Wen & Zhang, 2015). *Klebsiella* spp. employ the Wzx/Wzy driven route for the formation and surface presentation of CPS. This process involves the production of nucleotide sugar precursors specific to a particular K-type, followed by the assembly of the repetitive unit in the cytoplasmic area using sugar specific glycosyl transferases (GTs) (Shu et al., 2009; Patro & Rathinavelan, 2019). However, the process of LPS production and transfer to the outermost membrane of *Klebsiella* spp. is intricate, as it involves the formation of a lipid A, a core oligosaccharide, and a polysaccharide unit (Whitfield, 1995; Patro & Rathinavelan, 2019). The polysaccharide region, sometimes referred to as O-antigen, exhibits variation among different species of *Klebsiella* and is utilized for serotyping purposes. O-antigen production occurs in the cytosol using a similar process as CPS biosynthesis, involving the participation of many O-antigen specific GTs (Kos et al., 2009). Capsule typing, also known as K-typing, is frequently performed using the *wzi* or *wzc* genes found in the CPS biosynthesis gene cluster (Pan et al., 2015). Similarly, O-typing, which involves determining the O-antigen transport, often utilizes the *wzm* or *wzt* genes (Fang et al., 2016a; Follador et al., 2016). Because of their immunogenicity, these antigens can be used as targets for cutting-edge treatments like phage therapy and vaccine development. It's crucial to remember that there is a significant diversity of antigens in the population, and our knowledge of the prevalence and geographic distribution of different antigen types among different strains of disease-causing bacteria is still incomplete (M. M. C. Lam et al., 2022). The activation of the innate immune

system is due to the existence of *K. pneumoniae* capsular polysaccharide (K antigen) and lipopolysaccharide (O antigen), which are critical virulence factors (Simoons-Smit et al., 1984; Shankar et al., 2018). Furthermore, these two antigens are employed for the purpose of distinguishing *K. pneumoniae* isolates (Podschun & Ullmann, 1998). At present, the serotyping of *Klebsiella* spp. involves the utilization of 141 K-types and 13 O-types (Patro et al., 2020). *Klebsiella pneumoniae* capsule types exhibit significant variability in virulence characteristics. hvKp isolates are restricted to the following capsule types: K1, K2, K16, K28, K57, and K63. Specifically, K1 and K2 serotypes have been linked to almost 70% of all instances of hypervirulent *K. pneumoniae* (hvKp) infections recorded worldwide (Chung et al., 2007; W.-L. Yu et al., 2008; Marr & Russo, 2019). In contrast to the extremely variable K-antigens, which have more than 80 varieties, LPS is a less variable antigen that plays a crucial role in virulence. The structure of this compound includes lipid A, core oligosaccharide, and O-specific polysaccharide (O-PS, O-antigen), with the O-PS being responsible for identifying the O-serotype. While the O1-antigen is more common in clinical isolates of *K. pneumoniae* (Trautmann et al., 1997), it has been noted that the O2-antigen is more abundant in strains that are resistant to many drugs. Specifically, the subtype O2afg of the O2-antigen has been shown to provide better survival in human blood serum (Szijártó et al., 2016; Pennini et al., 2017). *K. pneumoniae* may be divided into two categories: classical strain and hypervirulent strain (Russo & Marr, 2019a). hvKP isolates often exhibit susceptibility to antibiotics, however they possess a very high level of virulence (Paczosa & Mecsas, 2016). HvKp was first identified in Taiwan in 1986 (Y. C. Liu et al., 1986), however genetic investigations indicate that it may have been present but undetected as far back as the 1920s (M. M. Lam et al., 2017). The hvKp strain is distinct from the cKp strain due to its possession of the *rmpA* and *rmpA2* mucoid regulator genes, as well as the K1, K2, K20 capsular types, and aerobactin (Russo et al., 2018). The hvKp strains have the potential to induce severe infections, including meningitis and liver abscess, in persons with both normal and weakened immune systems (Serban et al., 2021). *K. pneumoniae* is a concerning and renowned pathogen that has gained notoriety due to a growing prevalence of severe infections and a diminishing availability of effective therapeutic options. The emergence of *K. pneumoniae* strains exhibiting hypervirulence (HV) or resistance to antibiotics has resulted in the prevalence of these concerning situations.

Siderophores and mucoid regulators have been identified as the two kinds of components responsible for the hypervirulent phenotype (Shon et al., 2013; Patel et al., 2014). Bacteria release siderophores, which are chemicals used to capture iron. *K. pneumoniae* isolates have the ability to create a maximum of four siderophores. The genes that encode enterobactin (ent)

are present in nearly all strains of *K. pneumoniae.* However, the genes that encode salmochelin (iro) and aerobactin (iuc) are often found in hvKP strains. Yersiniabactin biosynthesis genes (*ybt*) may be found in some hypervirulent *K. pneumoniae* and classical *K. pneumoniae* isolates. These genes are often linked to the genes that produce the genotoxin colibactin (clb) and are incorporated into conjugative domains that is ICEKp10 (M. M. C. Lam et al., 2018). It's interesting to note that among these siderophores, enterobactin has the greatest affinity for iron and aerobactin the lowest (Tarkkanen et al., 1992; Koczura & Kaznowski, 2003). Unlike the other siderophores, enterobactin expression is well conserved between classical and hvKp strains. Therefore, enterobactin is likely the primary siderophore for iron absorption that *K. pneumoniae* employs (P. Hsieh et al., 2008; El Fertas-Aissani et al., 2013). Accurately distinguishing between hvKP and cKP strains is challenging, and there remains ongoing debate regarding the classifications of both categories (Harada & Doi, 2018). While hvKP strains are often associated with hypermucoviscous (hmv) feature, cKP strains might also possess it because of mutations within the capsule locus (wzc) (Ernst et al., 2020). hvKP has been characterized by several research as the mere existence of *iuc* genes (Y. Zhang et al., 2016; C. Liu, Du, et al., 2020).

In the Indian setting, there was a lack of comprehensive analysis of *K. pneumoniae*'s phenotypic test, which includes Sequence types, K-types, O-serotypes, String phenotype, drug resistance profile, and genetic structure. Therefore, this study utilized a selection of typical isolates, which will be advantageous in comprehending the mechanisms and associations, or lack thereof, between various virulence and resistance characteristics of *K. pneumoniae* isolates in India. The incorporation of mobile genetic elements has led to the emergence of highly virulent strains of *Klebsiella pneumoniae* (hvKp) that possess plasmids and integrative conjugative elements (ICEs) encoding essential virulence factors, including siderophores (aerobactin (iuc), yersiniabactin (ybt), and salmochelin (iro)), the colibactin toxin (clb), and/or genes responsible for a hypermucoviscosity phenotype (*rmpA/rmpA2*) (Wyres et al., 2016). Whole genome sequencing has significantly transformed the field of pathogen research by enabling the identification of antimicrobial resistance related mutations and plasmids (J. Phelan et al., 2016), as well as the analysis of evolutionary trees and transmission events (Napier et al., 2020). The *K. pneumoniae* phylogeny typically exhibits clades that align with the widely employed multi-locus sequence typing method, which relies on seven specific gene loci (Diancourt et al., 2005). Strains with distinct sequence types, K and O antigen types, and CGs can vary significantly in their ability to cause disease and their likelihood of being resistant to antibiotics (Bialek-Davenet et al., 2014). Tragically the often-employed *K. pneumoniae* MLST technique does not

provide the construction of a phylogeny with a high level of detail. The process of recombination and horizontal gene transfer within *K. pneumoniae* adds complexity to a phylogenetic study (Wyres et al., 2020), even when considering the same sequence types (Comandatore et al., 2019). In addition, a significant portion of the central genome shows less variation, while mobile genetic components, such as virulence and antimicrobial resistance genes, may have more clinical significance (Wyres et al., 2020).

This chapter primarily examined the genomic monitoring of highly pathogenic strains. The research identified the most prevalent K-type and O-type strains, their correlation with Sequence type, and the quantity of virulence genes present in their genomes. In addition, representative isolates were selected from the most common combinations in order to examine the phenotypic features, including determining capsule size, quantifying exopolysaccharides, assessing string phenotype, conducting phagocytosis and serum killing assays. Another research shown how the improper administration of antibiotics in cases of resistant isolates could trigger the formation of siderophores, which are substances of virulence in *K. pneumoniae*.

5.2 Materials and methodology

5.2.1 Pan-India *K. pneumoniae* genome data retrieval to study of virulence factors

A total of 351 genomes, including ours n = 29 (M2, M6, M10, M17B, M20, M25, M27, M33, M34a, M35, M36, M39, M40, M44, M47, M48, M49, M50, M51, M52, M53, M54, M55, M56, M57, M58, M59, DJ, and ST1) shown in **Figure 5.5** of *K. pneumoniae* from India, were obtained from the online tool PATRIC, a bioinformatics resource portal (https://www.patricbrc.org/) up to 25th October 2021, which has recently been combined with BV-BRC (https://www.bv-brc.org/). The genomes from India were accessed using filters such as 'India', and 'Genome quality: good'.

5.2.2 Bioinformatics analysis to detect Sequence types (STs), K-types, and O-types, and Virulence genes

Multi Locus Sequence Typing of all additional isolates were determined using methodology as mentioned in section 4.2.2. The identification of Capsular (K) and Lipopolysaccharide (O) types was accomplished by the utilization of Kaptive 2.0 tool with default parameter, available at https://kaptive-web.erc.monash.edu/. The process of identifying virulence genes involved doing a search for the most accurate matches using a virulence gene scheme, with the best

match for locus identification obtained from BIGSdb-Pasteur (https://bigsdb.pasteur.fr/klebsiella/).

5.2.3 Generation of a phylogenetic tree based on SNPs using WGS data

A phylogenetic tree was created using CSI Phylogeny 1.4 software, which is based on single nucleotide polymorphisms (SNPs) for virulence data. The software may be accessed at https://cge.food.dtu.dk/services/CSIPhylogeny/. The parameter specified a minimum depth of 10x at SNP positions, a minimum SNP quality of 30, a minimum relative depth of 10% at SNP positions, and a minimum Z-score of 1.96. The reference strain MGH 78578 (GenBank: CP000647.1) had been used for this analysis. Additionally, tree data collected in Newick format was uploaded to the iTOL program (https://itol.embl.de/itol.cgi) for visualization purposes. The annotated and assembled data of STs, K-type, O-type, and virulence genes were then linked to the iTOL image as shown in **Figure 5.5**.

5.2.4 Selection of isolates for phenotypic study of Capsule and lipopolysaccharides

5.2.4.1 String test

To determine the hypermucoviscous trait, string test was carried out. The bacteria were cultured overnight at 37°C on agar plate supplemented with 5% sheep blood (Himedia, India). A mucosal bacterial colony was then stretched using a bacteriological inoculation loop. A positive HMV phenotype was indicated by the presence of a string longer than 5 mm (J. Wang et al., 1998; Shon et al., 2013). An additional string positive isolate (M20) was used in this analysis to duplicate the sole string positive isolate (M58) that was first detected. To facilitate subsequent research, representative isolates were further chosen based on the predominance of STs, K-type, O-type in Pan-India genome analysis, and String test were also taken into consideration while picking our isolates, which were shown in a **Table 5.1**.

Table 5.1 *K. pneumoniae* isolates selected for the phenotypic study of capsule and lipopolysaccharide.

Isolates	Sequence type	K-type	O-type	String test
M17B	ST14	K2	O2a	-ve
M48	ST2096	K64	O1	-ve
M49	ST147	K64	O2a	-ve
DJ	ST147	K64	O2a	-ve
M50	ST231	K51	O1	-ve
M51	ST231	K51	O1	-ve
M57	ST231	K51	O1	-ve
M58	ST11	K24	O2a	+ve
M20	ST2943/ST2	K39	O3b	+ve

5.2.4.2 Capsule staining and size determination

The capsule was subjected to staining using Maneval's staining procedure (Hughes et al., 2017) and subsequently observed using a light microscope at a magnification of 100X employing oil immersion. Overall size of the capsule was calculated using Image J software, with a minimum of 100 cells being analyzed.

5.2.4.3 Mucoviscosity Assay

The mucoviscosity assay was conducted using the previously outlined protocol (Y. Zhang et al., 2016). Bacterial isolates were grown in Luria Bertani Broth (L.B.) at 37°C for 6 hours with constant shaking. The optical density (OD) at 600nm was normalized to OD 1.0 for each isolate after incubation. Next, 1mL of each isolate was centrifuged at 1000xg for 5 minutes. Each isolate's OD_{600} was then measured. Pelleting mucoviscous isolates was more difficult leading to supernatants that had greater absorbance (Russo et al., 2018).

5.2.4.4 FITC labelling of bacterial isolates

Bacteria were FITC labelled using the previously published protocol (L. Wang et al., 2017) with a few minor adjustments. Overnight at 37°C, bacteria isolates were cultivated in Luria Bertani broth and adjusted using a spectrophotometer to an initial OD600 = 0.2. For sixty minutes, the bacteria were kept in a water bath at 70˚C. After killing the bacteria, they were rehydrated in 0.1 M $NaHCO_3$, pH 9.0, at 25˚C for an hour, and labelled with fluorescein isothiocyanate [FITC (0.1 mg/ml); Sigma Chemical Co.]. Three times, PBS was used to wash out unbound FITC. After being aliquoted and kept at 4˚C, FITC-labelled bacteria were

resuspended in PBS at a concentration of 2 × 10^8 cells/ml. The bacterial cells were then observed in 100x magnification under the microscope **(Figure 5.1)**.

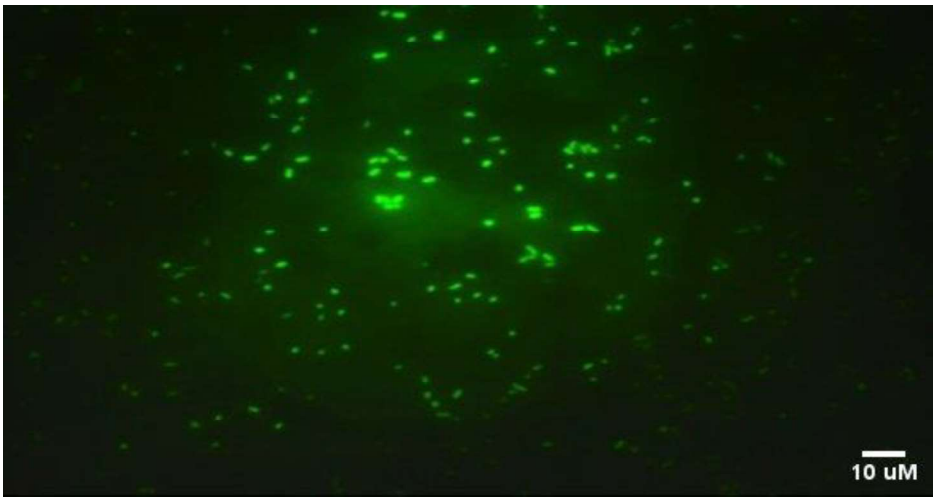

Figure 5.1 Representative image of the FITC-labeled isolate M51 under 100x magnification. The bacterial cells stained with a green-fluorescent dye against a dark background.

5.2.4.5 Isolation of human WBC from whole blood

In an EDTA vacutainer, 5 mL of whole blood was extracted. At 20^0 Celsius, the entire blood sample was centrifuged for 10 minutes at 500xg. After discarding the yellow supernatant, blood was mixed with 3 mL of PBS and centrifuged at 1000xg for 15 minutes at 20°C. After discarding the colourless supernatant, 8mL of 1X RBC lysis buffer was added to the solution. The mixture was incubated at 37°C for 10 minutes. Next, the solution was centrifuged at 20°C for 10 minutes with a force of 1000xg, ten times the acceleration due to gravity. For complete red blood cell destruction, RBC lysis was repeated. The solid residue was washed with phosphate-buffered saline after removal of liquid. The pellet was reconstituted in PBS to reach a final concentration of 1×10^7 cells per millilitre.

5.2.4.6 Flow cytometric analysis of phagocytosis

The experimental setup used a FACScan equipment with a 488 nm argon laser. FITC fluorescence was detected using this setup. Forward scatter (FSC), sideway scatter (SSC), and fluorescence 1 (FLH-1, green) detector settings were E00, 350, and 427, respectively. The SSC threshold was 52. After gating the detector, fluorescence measurements were taken using FSC and SSC. The threshold for positive and negative fluorescence was determined by analysing bacterium mixtures stained with FITC and unstained. Histograms of FL1-H fluorescence

distribution data were shown. The number of events processed for each sample was 10,000. This study only included granulocytes as a population. We ensured comparability through analysis of all samples under the same settings. The FACS data was evaluated using Flowing software v2.5.1.

5.2.4.7 Serum Killing Assay

A total of five individuals voluntarily contributed their blood samples for the study, which was then combined. Five millilitres of blood was drawn from each healthy individual and placed in fifteen millilitre falcon tubes. For two hours, blood was left to clot at room temperature. At 4°C for 10 minutes, 2000x g centrifugation was performed. Serum was isolated from the clot after centrifugation, aliquoted into 1.5 mL tubes, and kept at -20°C. A 25 µL inoculum was taken from the mid-log phase with an OD600 range of 0.08-0.10. After diluting the inoculum with 0.9% normal saline, 75 µL of pooled human serum was added. To assess colony count, serial dilutions were conducted and plated on Mueller-Hinton agar (MHA) medium at 0, 1, 2, and 3 hours. A microtiter plate was used to generate dilutions by mixing 90µL of normal saline with 10µL of the sample. A 30µL amount was selected from the final dilution and equally applied on MHA plate. Plates were incubated at 37 ^{0}C. At least three tests were conducted on each strain, and the average outcomes were reported as a percentage of inoculums. As previously mentioned, the responses were graded from 1 to 6 in terms of viable counts, and the findings were reported as a percentage of inoculation (Abate et al., 2012). Serum sensitivity was characterized as grades 1-2, intermediate sensitivity as grades 3-4, and resistance as grades 5-6 for a strain.

5.2.5. Qualitative and Quantitative detection of siderophore

5.2.5.1 Qualitative detection of siderophore

The protocol is comprehensive, sequential methodology derived from (Schwyn & Neilands, 1987). Thoroughly cleansed all glassware using a solution of 6 M hydrochloric acid (HCl) to eliminate any residual components, followed by a rinse with deionized water (ddH_2O). The first stage in preparing 1 liter of CAS medium involved preparing a blue dye. To make the (A) blue dye, three solutions must be prepared: Solution 1 required dissolving around 0.06 grams of CAS (Himedia, India) in 50 milliliters of double-distilled water. Solution 2 entailed dissolving approximately 2.7 milligrams of $FeCl_3.6H_2O$ in 10 milliliters of 10 millimolar hydrochloric acid (10 mM HCl). Lastly, Solution 3 involved dissolving approximately 0.073 grams of hexadecyltrimethylammonium bromide (HDTMA) in 40 milliliters of double-

distilled water. Next, we blended 9 ml of Solution 2 with Solution 1. Subsequently, I combined it with Solution 3 and observed the formation of a blue color in the solution. Then the blue dye was placed in an autoclave for sterilization and thereafter stored in a plastic container or bottle. (B) a mixture solution was created as the next phase, consisting of four sub-steps. In the first sub-step, we prepared a Minimal Media 9 (MM9) Salt Solution Stock by dissolving 15 g of KH_2PO_4, 25 g of NaCl, and 50 g of NH_4Cl in 500 ml of ddH_2O. In the second phase, a 20% Glucose Stock was prepared by dissolving 20 grams of glucose in 100 milliliters of ddH_2O. The third stage included the preparation of NaOH Stock by dissolving 25 g of NaOH in 150 ml of distilled water (ddH2O). The desired pH level should be about 12. Lastly, prepared the Casamino Acid Solution by dissolving 3 grams of Casamino acid (Sisco Research laboratories Pvt. Ltd., Mumbai, India) in 27 milliliters of ddH_2O. Then, extracted the solution with 3% 8-hydroxyquinoline in chloroform to eliminate any remaining residues. Additionally, sterilization may be achieved by filtration using a 0.22-micron filter paper. (C) In the last stage of CAS agar preparation, 100 ml of MM9 salt solution was combined with 750 ml of ddH_2O. Then, 32.24 g of piperazine-N, N'-bis (2-ethanesulfonic acid) PIPES (Himedia, India) was dissolved and stirred at a pH of 6.8. Afterwards, 15 grams of Bacto agar was added and then subjected to autoclaving. The mixture was then cooled down to a temperature of 50 ^{0}C. Next, 30 ml of sterile Casamino acid solution and 10 ml of sterile 20% glucose solution were mixed into the MM9/PIPES mixture. Gradually, 100 ml of Blue Dye solution was introduced into the mixture while ensuring sufficient agitation to achieve thorough mixing. Further, each bacterial strain was put onto plates. A plate without any inoculation was used as a control. Following inoculation, the plates were placed in an incubator at a temperature of 28 °C for a period of 5 to 7 days. During this time, the plates were monitored for the development of an orange/yellow zone around the bacterial colonies (Louden et al., 2011).

5.2.5.2 Quantitative detection of siderophore by modified microplate method

The measurement of siderophore was performed using the Modified microplate technique described by (Arora & Verma, 2017). Concisely, the supernatant was acquired by placing it in a microcentrifuge tube from a 0.5 ml broth sample that was inoculated for 48 hours at 28 °C with 5 µl of inoculum containing 10^8 cfu/ml. 100 µl of supernatant from each bacterial culture was added to individual wells of a sterile microplate, followed by the addition of 100 µl of CAS reagent in liquid form. Following incubation of 20-30 minutes at room temperature, the optical density of each sample, which was put in the wells of a microplate, was measured at a

wavelength of 630 nm using a microplate reader (Thermo Scientific Multiskan GO, USA). Four replicates were obtained for each strain on a 96-well plate, The siderophore generated by the strains was quantified in percent siderophore units (psu), using the calculation method described by (Payne, 1993): Siderophore production (psu)= (Ar-As) x 100 / Ar, where the variable Ar represents the absorbance of the reference, which includes the CAS solution and un-inoculated broth. The variable as represents the absorbance of the sample, which includes the CAS solution and the cell-free supernatant of the sample.

5.2.5.3 Study on effect of Iron, DIP (Iron Chelator) and antibiotics on %siderophore production

To investigate the impact of iron, and iron chelator 2.,2' dipyridyl (DIP), and antibiotics (ampicillin, ciprofloxacin, and colistin), were used to assess their effectiveness against six distinct isolates M10 (MDR), M33 (Susceptible), M48 (XDR), M50 (PDR), M51 (XDR), and M52 (XDR) of *K. pneumoniae* based on their resistance and genomics profile for siderophore genes as mentioned in **Table 3.4, Figure 5.5 & 5.13**. The selection of isolates was based on their genomic profile for siderophore genes and their drug resistance category. In order to conduct the research, all samples thrived in ideal conditions in LB broth with varying doses of iron (100uM, 50 µM, 25 µM), and DIP (400uM, 200 µM, 100 µM) individually for each variable as described in (Washington – Hughes et al., 2019; T. Chen et al., 2020). For the antibiotics, concentrations that were one-fold higher than the minimum inhibitory concentration (MIC), as well as those that were one-fold and two-fold lower than the MIC, were chosen. All samples were cultured in the presence of different concentrations of ampicillin (40 ug/ml, 20 ug/ml, 10 ug/ml, 5 ug/ml), ciprofloxacin (10 ug/ml, 5 ug/ml, 2.5 ug/ml, 1.25 ug/ml), and colistin (2.5 ug/ml, 1.25 ug/ml, 0.625 ug/ml, 0.312 ug/ml) individually for each variable. After incubating all the tubes for 24 hours, the optical density (OD) was measured at 600 nm to determine the growth rate. The production of siderophore was also detected, and the percentage of siderophore was calculated using the modified microplate technique described in section 5.2.5.2.

5.3 Results

5.3.1 Overall summary of ST, K- and O-locus, and virulence genes among genomes.

There were 93 different sequence types detected among the genomes (*n* = 351) of *Klebsiella pneumoniae* of which ST231 (*n* = 105; 29.91%) was the predominant followed by ST14 (*n* = 37; 10.54%), ST147 (*n* = 27; 7.69%), ST2096 (*n* = 21; 5.98%), and ST11 (*n* = 10; 2.84%) as shown in **Figure 5.2** and **5.5.** Across the genomes of *Klebsiella*, 43 different K-types and 13 different O-types were detected as shown in **Figure 5.5**, of which K51 (*n* = 112; 31.9%) was the highest followed by K64 (*n* = 52; 14.81%), K2 (*n* = 37; 10.54%), and K10 (*n* = 14, 3.98%) in K-type (**Figure 5.3**), and O1 (*n* = 214; 60.96%) was the most circulating in O-types followed by O3/O3a (*n* = 37; 10.54%), O2a (*n* = 35; 9.97%), O3b (*n* = 19; 5.41%), and O2afg (*n* = 17; 4.84%) as shown in **Figure 5.4**. In the case of virulence genes, a total of 44 different kinds of virulence genes were detected throughout genomes of *K. pneumoniae*, of which genes related to biofilm/type-3 fimbriae *mrkABCDFHIJ* were most circulating (87.46%–93.73%), followed by genes *fyuA*, *irp1*, *irp2*, and *ybtAEPQSTUX* related to yersiniabactin (Ybt) biosynthesis (55.3%–70.37%), gene *kfuABC* related to ferrus ion uptake (44.16%–60.68%), and gene related to aerobactin transport *iutA* and synthesis *iucABCD* (27.07%–74.6%).

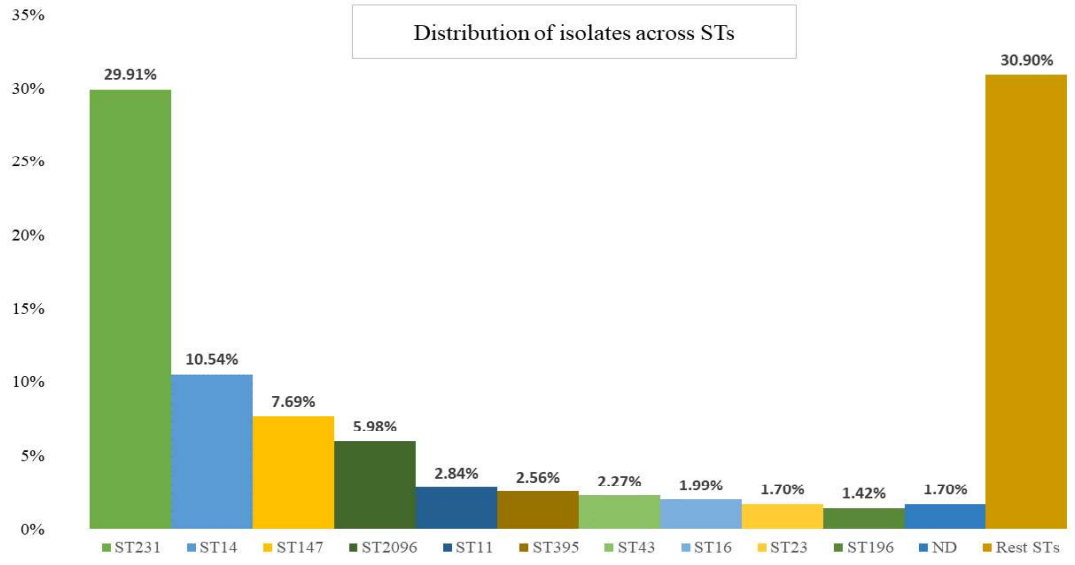

Figure 5.2 Dispersion of sequence types throughout the genomes of *K. pneumoniae*. ST231 had the greatest frequency, almost 30%, followed by ST14, ST147, ST2096, and a few others.

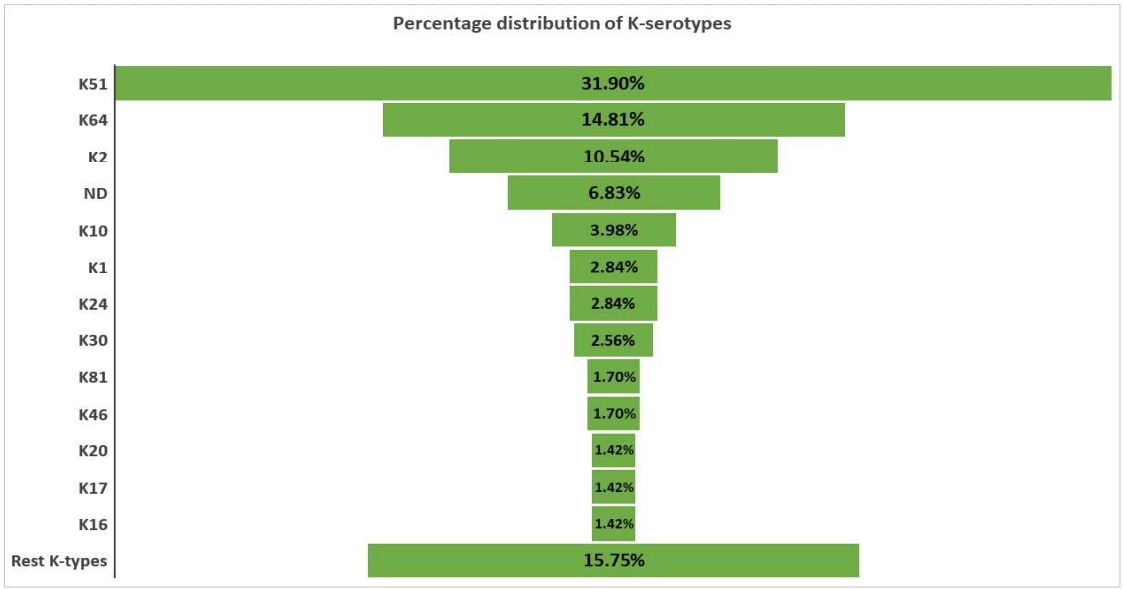

Figure 5.3 Distribution of K-types across *K. pneumoniae's* genomes. K51 had the greatest frequency, around 31%, followed by K64, K2, whereas K20, K17, and K16 were less common across genomes.

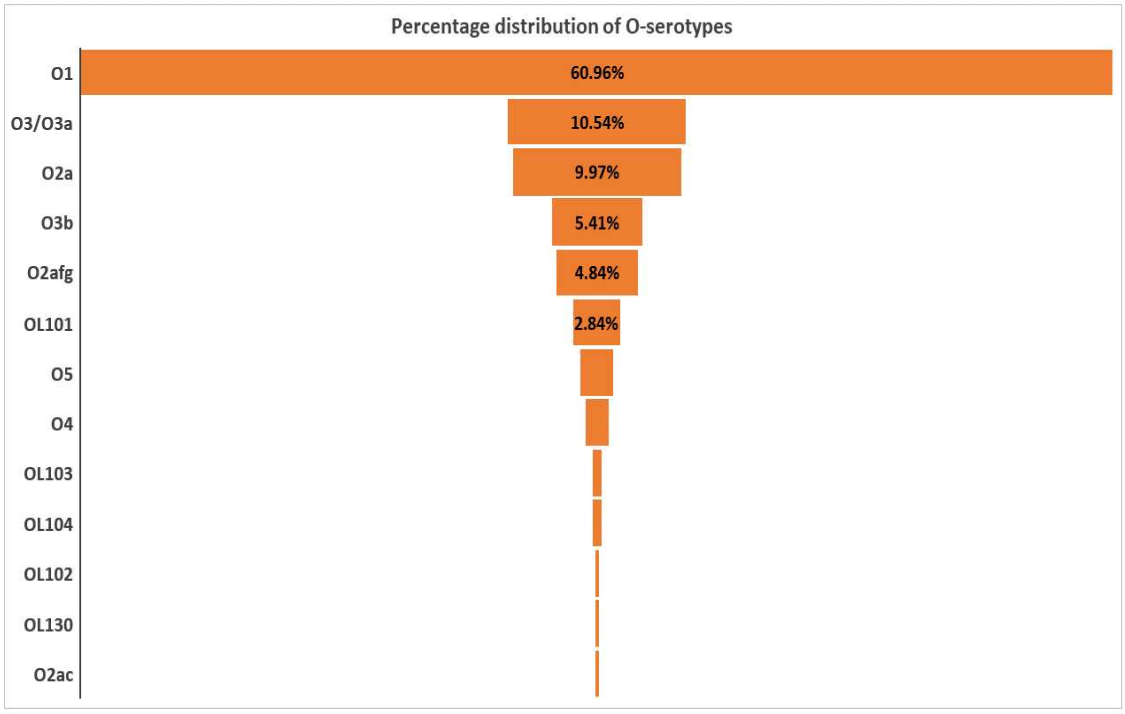

Figure 5.4 Distribution of O-serotypes across *K. pneumoniae's* genomes. O1 had the greatest frequency, around 61%, followed by O3/O3a, O2a, while OL102, OL130, and O2ac were the lowest.

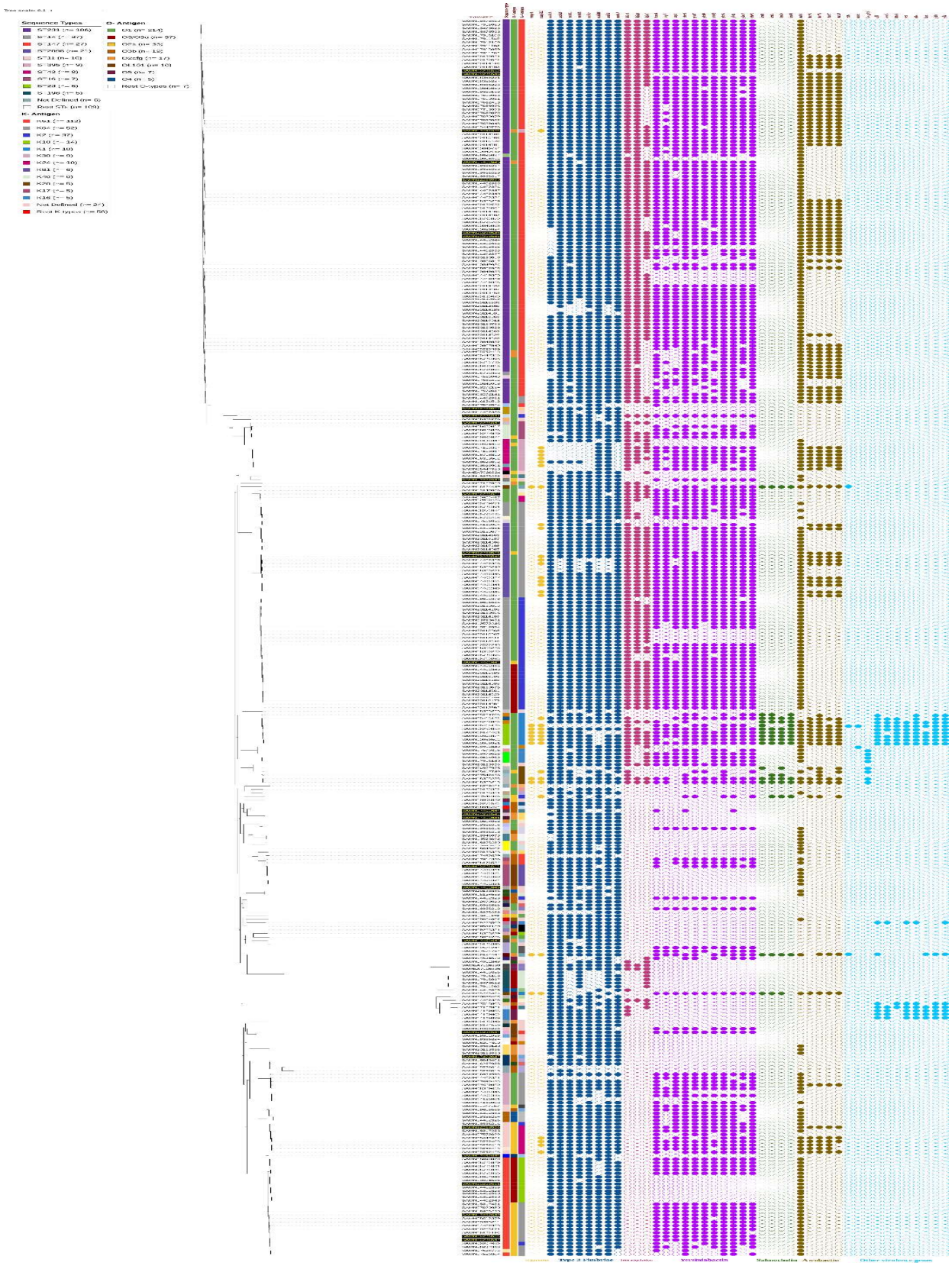

Figure 5.5 A complete genetic profile of the virulence of *K. pneumoniae* genomes from India. The tree is based on single nucleotide polymorphisms (SNPs). The graphic displays the biosamples, namely the lab isolates marked in yellow, together with their sequence types, K-type, O-type, and the virulence genes associated with each isolate.

5.3.2 Correlation of major prevalent STs with K-type, O-type, and Virulence genes among *K. pneumoniae* genomes (*n* = 351)

A total of 11 frequent ST types (ST231, ST14, ST147, ST2096, ST11, ST395, ST43, ST16, ST23, and ST196), 9 K-types (K51, K64, K2, K10, K24, K30, K81, K1, and K46), and 5 O-types (O1, O2afg, O3/O3a, O2a, and OL101) were assembled to demonstrate their relationship to one another, as seen in **Figure 5.6**.

5.3.2.1 ST231

In ST231 (*n* = 105), near to all isolates belonged to K51-type (98.09%) and O1-type (96.19%) except a few isolates, which belonged to K64 and O2afg. K51 + O1 were highly predominant in ST231 and contributed to *n* = 99; 94.28%, another combination of K51-type and O2afg-type were also detected *n* = 4; 3.80%. Most of the ST231(K51 + O1) and ST231(K51 + O2afg) had *mrkABCDFHIJ* gene cluster. Gene *mrkH* was the most frequent among ST231 isolates and detected in all ST231 (K51 + O1) isolates (100%), while *mrkA* was the least frequent from *mrk* gene cluster among ST231(K51 + O1) isolates (87.88%). Whereas in ST231(K51 + O2afg) all *mrk* genes except *mrkD* were present in all isolates. The genes *rmpA* and *rmpA2* were absent in all isolates of ST231. The ferric uptake operon *kfuABC* genes, *kfuA* and *kfuB* were highly prevalent in both the ST231(K51 + O1) and ST231(K51 + O2afg) and detected in all genomes except one that lacks *kfuB*, interestingly *kfuC* that was only detected in *n* = 65; 65.65% of ST231(K51 + O1) and *n* = 2; 50% of ST231(K51 + O2afg) genomes. The presence of the yersiniabactin biosynthetic genes *fyuA, irp1* & *irp2*, and *ybtAEPQSTUX* in ST231 ranged from 79.04% to 94.28%. It is interesting to note that only *ybtA* (93.33%) and *ybtT* (89.52%) were found in duplicates, with the rest still existing in single copies. Additionally, gene *ybtA* (*n* = 99; 94.28%) was the most frequent in the genomes, while *irp1* (*n* = 83; 79.04%) and *irp2* (*n* = 84; 80%) were the least abundant. In ST231(K51 + O1) and ST231(K51 + O2afG), all the Ybt synthesis genes were distributed in similar manners. There was no salmochelin gene cluster *iroBCDN* detected in any of the ST231 genomes. The *iutA* gene responsible for aerobactin transport was detected in all genomes (*n* = 105; 100%) of ST231 of them *n* = 49; 46.66% were in duplicate, However, only around half of the genomes contained the *iucABCD* genes, which are necessary for the synthesis of aerobactin. In genomes of ST231(K51 + O1), *n* = 51; 51.51% genomes contained *iucABC* while *n* = 50; 51.50% genomes contained *iucD*. In *n* = 3; 75% of ST231(K51+ O2afG) genomes, *iucABCD* was present. It is interesting to note that, among the ST231 genomes, the aerobactin synthesis genes *iucABCD* were primarily found (*n* =48/56; 85.71%) in genomes with a dual copy of the *iutA* gene.

Virulence factors	ST231 (K51, O1); n= 99	ST231 (K51, O2afg); n= 4	ST14 (K2, O1); n= 18	ST14 (K2, O3/O3a); n= 13	ST14 (K64, O1); n= 4	ST147 (K64, O2a); n= 13	ST147 (K10, O3/O3a); n= 13	ST2096 (K64, O1); n= 20	ST11 (K24, O2a); n= 7	ST395 (K64, O1); n= 9	ST43 (K30, O1); n= 7	ST16 (K81, OL101); n= 6	ST23 (K1, O1); n= 6	ST196 (K46, O3/O3a); n= 5
rmpA	0.0%	0.0%	0.0%	0.0%	0.0%	0.0%	0.0%	0.0%	0.0%	0.0%	0.0%	0.0%	100.0%	0.0%
rmpA2	0.0%	0.0%	0.0%	0.0%	0.0%	0.0%	0.0%	50.0%	57.1%	0.0%	71.4%	0.0%	100.0%	0.0%
mrkA	87.9%	100.0%	100.0%	100.0%	100.0%	92.3%	100.0%	100.0%	100.0%	88.9%	28.6%	100.0%	83.3%	100.0%
mrkB	99.0%	100.0%	100.0%	100.0%	100.0%	100.0%	100.0%	80.0%	100.0%	88.9%	28.6%	100.0%	83.3%	100.0%
mrkC	93.9%	100.0%	100.0%	100.0%	100.0%	100.0%	100.0%	100.0%	100.0%	88.9%	28.6%	100.0%	83.3%	0.0%
mrkD	93.9%	75.0%	100.0%	100.0%	100.0%	100.0%	92.3%	80.0%	100.0%	66.7%	28.6%	100.0%	83.3%	100.0%
mrkF	99.0%	100.0%	100.0%	100.0%	100.0%	100.0%	100.0%	95.0%	100.0%	77.8%	14.3%	100.0%	66.7%	0.0%
mrkH	100.0%	100.0%	100.0%	100.0%	100.0%	92.3%	69.2%	80.0%	100.0%	44.4%	85.7%	83.3%	16.7%	0.0%
mrkI	97.0%	100.0%	100.0%	100.0%	100.0%	100.0%	100.0%	80.0%	100.0%	77.8%	100.0%	100.0%	66.7%	100.0%
mrkJ	99.0%	100.0%	100.0%	100.0%	100.0%	92.3%	92.3%	100.0%	100.0%	77.8%	14.3%	100.0%	66.7%	80.0%
kfuA	100.0%	100.0%	100.0%	100.0%	100.0%	0.0%	0.0%	100.0%	0.0%	0.0%	100.0%	0.0%	100.0%	0.0%
kfuB	99.0%	100.0%	83.3%	100.0%	25.0%	0.0%	0.0%	95.0%	0.0%	0.0%	85.7%	0.0%	83.3%	0.0%
kfuC	65.7%	50.0%	72.2%	100.0%	0.0%	0.0%	0.0%	95.0%	0.0%	0.0%	57.1%	0.0%	66.7%	100.0%
fyuA	90.9%	75.0%	77.8%	100.0%	100.0%	92.3%	38.5%	100.0%	100.0%	88.9%	85.7%	16.7%	100.0%	0.0%
irp1	79.8%	50.0%	61.1%	100.0%	100.0%	92.3%	38.5%	95.0%	57.1%	55.6%	57.1%	0.0%	83.3%	0.0%
irp2	80.8%	50.0%	66.7%	100.0%	75.0%	84.6%	38.5%	85.0%	71.4%	77.8%	85.7%	0.0%	83.3%	0.0%
ybtA	93.9%	100.0%	77.8%	100.0%	100.0%	100.0%	38.5%	100.0%	100.0%	100.0%	85.7%	16.7%	83.3%	0.0%
ybtE	90.9%	75.0%	77.8%	100.0%	100.0%	92.3%	38.5%	65.0%	85.7%	77.8%	85.7%	16.7%	100.0%	0.0%
ybtP	82.8%	100.0%	66.7%	100.0%	100.0%	84.6%	38.5%	95.0%	100.0%	77.8%	85.7%	16.7%	100.0%	0.0%
ybtQ	84.8%	75.0%	72.2%	100.0%	50.0%	84.6%	38.5%	95.0%	71.4%	77.8%	71.4%	16.7%	66.7%	0.0%
ybtS	91.9%	100.0%	77.8%	100.0%	100.0%	100.0%	38.5%	100.0%	100.0%	77.8%	85.7%	16.7%	100.0%	0.0%
ybtT	92.9%	100.0%	77.8%	100.0%	100.0%	100.0%	38.5%	100.0%	100.0%	66.7%	85.7%	16.7%	100.0%	0.0%
ybtU	84.8%	100.0%	72.2%	100.0%	75.0%	84.6%	38.5%	95.0%	85.7%	55.6%	71.4%	16.7%	100.0%	0.0%
ybtX	91.9%	100.0%	77.8%	100.0%	100.0%	92.3%	38.5%	100.0%	100.0%	77.8%	85.7%	16.7%	83.3%	0.0%
iroB	0.0%	0.0%	0.0%	0.0%	0.0%	0.0%	0.0%	0.0%	0.0%	0.0%	0.0%	0.0%	100.0%	0.0%
iroC	0.0%	0.0%	0.0%	0.0%	0.0%	0.0%	0.0%	0.0%	0.0%	0.0%	0.0%	0.0%	83.3%	0.0%
iroD	0.0%	0.0%	0.0%	0.0%	0.0%	0.0%	0.0%	0.0%	0.0%	0.0%	0.0%	0.0%	83.3%	0.0%
iroN	0.0%	0.0%	0.0%	0.0%	0.0%	0.0%	0.0%	0.0%	0.0%	0.0%	0.0%	0.0%	100.0%	0.0%
iutA	100.0%	100.0%	100.0%	100.0%	50.0%	100.0%	100.0%	95.0%	85.7%	77.8%	100.0%	83.3%	100.0%	0.0%
iucA	51.5%	75.0%	0.0%	0.0%	0.0%	0.0%	0.0%	50.0%	71.4%	11.1%	85.7%	0.0%	100.0%	0.0%
iucB	51.5%	75.0%	0.0%	0.0%	0.0%	0.0%	0.0%	50.0%	71.4%	11.1%	85.7%	0.0%	100.0%	0.0%
iucC	51.5%	75.0%	0.0%	0.0%	0.0%	0.0%	0.0%	50.0%	71.4%	11.1%	71.4%	0.0%	100.0%	0.0%
iucD	50.5%	75.0%	0.0%	0.0%	0.0%	0.0%	0.0%	50.0%	57.1%	11.1%	85.7%	0.0%	100.0%	0.0%
clb	0.0%	0.0%	0.0%	0.0%	0.0%	0.0%	0.0%	0.0%	0.0%	0.0%	0.0%	0.0%	16.7%	0.0%
mce	0.0%	0.0%	0.0%	0.0%	0.0%	0.0%	0.0%	0.0%	0.0%	0.0%	0.0%	0.0%	16.7%	0.0%
kvgAS	0.0%	0.0%	0.0%	0.0%	0.0%	0.0%	0.0%	0.0%	0.0%	0.0%	0.0%	0.0%	0.0%	0.0%
all	0.0%	0.0%	0.0%	0.0%	0.0%	0.0%	0.0%	0.0%	0.0%	0.0%	0.0%	0.0%	100.0%	0.0%
arcC	0.0%	0.0%	0.0%	0.0%	0.0%	0.0%	0.0%	0.0%	0.0%	0.0%	0.0%	0.0%	83.3%	0.0%
fdrA	0.0%	0.0%	0.0%	0.0%	0.0%	0.0%	0.0%	0.0%	0.0%	0.0%	0.0%	0.0%	100.0%	0.0%
gcl	0.0%	0.0%	0.0%	0.0%	0.0%	0.0%	0.0%	0.0%	0.0%	0.0%	0.0%	0.0%	100.0%	0.0%
glx	0.0%	0.0%	0.0%	0.0%	0.0%	0.0%	0.0%	0.0%	0.0%	0.0%	0.0%	0.0%	100.0%	0.0%
hyi	0.0%	0.0%	0.0%	0.0%	0.0%	0.0%	0.0%	0.0%	0.0%	0.0%	0.0%	0.0%	83.3%	0.0%
ybb	0.0%	0.0%	0.0%	0.0%	0.0%	0.0%	0.0%	0.0%	0.0%	0.0%	0.0%	0.0%	100.0%	0.0%
ylb	0.0%	0.0%	0.0%	0.0%	0.0%	0.0%	0.0%	0.0%	0.0%	0.0%	0.0%	0.0%	100.0%	0.0%

Figure 5.6 Percentage distribution of virulence genes across various combinations of prevalent STs (K-types, O-types). In this figure a combination of ST231 (K51, O1) was the highest with *n* = 99 isolates whereas ST231 (K51, O2afg) and ST14 (K64, O1) was the lowest with *n* = 4 isolates each. However, the greatest number of virulence genes were detected in a combination of ST23 (K1, O1).

5.3.2.2 ST14

In ST14 (*n* =37), three different K-type (K2, K51, and K64) and three different O-type (O1, O2a, and O3/O3a) were found, with K2 + O1 having the greatest combination (*n* =18; 48.64%), followed by K2 + O3/O3a (*n* =13; 35.13%) and K64 + O1 (*n* =4; 10.81%). Both *rmpA* and *rmpA2* were absent in all ST14. Regardless of K-type or O-type, all ST14 genomes have all *mrkABCDFHIJ* genes, except for one ST14(K51 + O1) genome that only lacks the *mrkA* gene. Aside from two ST14 genomes, *mrkC* duplication were found in all ST14 genomes. All ST14 genomes had the ferric uptake gene *kfuA*; however, *kfuB* and *kfuC* were found in ST14(K2 + O1) and ST14(K64 + O1), respectively, with frequencies of 83.33% and 72.22% and 25% and 0%, respectively. It's interesting to note that all ST14(K2 + O3/O3a) genomes had all three *kfuA*BC genes. Ybt synthesis genes *fyuA*, *irp1* & *irp2*, and *ybtAEPQSTUX* were observed in all ST14(K2 + O3/O3a) and ST14(K64 + O1) genomes except *irp2* (75%), *ybtQ* (50%), and *ybtU* (75%) in the genomes of ST14(K64 + O1), whereas the distribution of Ybt synthesis genes was below 80% in ST14(K2 +O1) genomes. Across ST14 genomes, nearly all *ybtA* (96.96%) and *ybtT* (90.90%) were found in duplicate. Except for two genomes, a majority of ST14 genomes (*n* =35, 94.59%) carried the aerobactin transport gene *iutA*. Interestingly, none of the ST14 genomes had the *iucABCD* genes, apart from a unique ST14 combination (K51 + O1).

5.3.2.3 ST2096

Except for a particular ST2096 combination (K64 + O2a), all the genomes in ST2096 (*n* = 21) belonged to the K64-type and the O1-type. Gene *rmpA* was absent from all the genomes, however *rmpA2* was found in (*n* =10, 47.61%) of the ST2096 genomes and all were belonged to K64 + O1 combination. The distribution of the mrk genes in ST2096 (K64 +O1) genomes showed diversity; the three genes *mrkA*, *mrkC*, and *mrkJ* were found in every genome (100%) followed by *mrkF* (95%) and *mrkBDHI* (80%). Considering the exception of one genome that lacks *kfuB*C genes, all three *kfuABC* genes were present in the ST2096 genomes. In the Ybt Synthesis Genes, *fyuA* and *ybtASTX* genes were circulating in all genomes of ST2096, while others, *irp1*, *irp2*, and *ybtEPQU*, ranged between 66.67% and 95.23%. Notably, *ybtE* was the least prevalent gene overall, while double copies of the *ybtA* and *ybtT* genes were found across the ST2096 genomes. The *iutA* gene was present in the genomes of all ST2096 isolates except for one; *n* = 10 of these isolates had two copies of the *iutA* gene. Surprisingly, only isolates with two copies of the *iutA* gene possessed the *iucABCD* genes in their genomes

5.3.2.4 ST147

Two primary K-type and O-type pairings were observed in the ST147 (*n* = 27) genome: K64 + O2a (*n* = 13; 48.14%) and K10 + O3/O3a (*n* = 13; 48.14%). All the ST147 genomes lacked the *rmpA* and *rmpA2* genes. In type 3 fimbriae (mrk) genes, *mrkBCFI* found in every genome of ST147, whereas *mrkADHJ* were absent in a small number of isolates and ranged from 81.48% to 96.29%. The majority of *mrkC* was found to have two copies (88.88%), which is noteworthy. Except for *mrkH*, which was much less common (69.23%) in K10 + O3/O3a, the distribution of other mrk genes was almost similar in K64 + O2a and K10 + O3/O3a. Surprisingly, none of the ST147 genomes had *kfuA*BC genes. In ST147 (K10 + O3/O3a) combination, the ybt genes *fyuA*, *irp1* & 2, and *ybtAEPQSTUX* were found in only 5 genomes (38.46%) compared to ST147 (K64 + O2a), which ranged from 84.61% to 100%. Interestingly, ST147 (K10 + O3/O3a) genomes showed all two copies of the *ybtA* gene, apart from one. All ST147 genomes carried the *iutA* gene, but strangely, none of them contained the *iucABCD* genes.

5.3.2.5 ST11, ST395, ST43, ST16, ST23, ST196, and ST101

In Pan-India *K. pneumoniae* genomes, *n* =10 ST11 genomes were found, and of those, 70% belonged to K24 + O2a. All isolates lacked *rmpA*, however 40% of isolates had *rmpA2* present. Interestingly, double copies of *mrkA* and *mrkC* appeared in 90% of isolates. All mrk genes, *mrkABCDFHIJ*, were identified in all isolates. The majority of the Ybt genes, *fyuA* and *ybtAPSTX*, were found in all isolates, while others were found in a range of 60–90% of isolates, with *irp2* being the least common (60%). Gene *iucABCD* ranged from 40–50% across the genomes, while *iutA* was found in 80% of isolates.

A total of nine genomes were identified as ST395, with each genome exhibiting a combination of K64 and O1. Across the genomes of ST395, 88.88% genomoes had *mrkABC* genes, 77.77% had *mrkFIJ* genes, while *mrkD* and *mrkH* was detected in 66.66% and 44.44% of genomes respectively. Both *mrkA* and *mrkC* strongly coappeared in term of dual copy and detected in 66.66% of genomes. Gene *ybtA* was detected in all isolates, while other Ybt genes *fyuA*, *irp1*, *irp2*, and *ybtEPQSTUX* were ranged between 55.55%-88.88% with *irp1* and *ybtU* as least (55.55%) prevalent. Gene *iutA* was frequently observed with 77.77% prevalence while genes *iucABCD* were detected only in 11.11% genomes.

Among ST43 (*n* = 8), K30 and O1 was the most common (*n* = 7; 87.5%) combination detected, of which 71.42% genomes had *rmpA2* gene. Interestingly, only *mrkI* was detected in all isolates followed by *mrkH* (87.5%), *mrkABCD* (25%), and *mrkFJ* (12.5%). *kfuA* was detected in all

isolate, followed by *kfuB* (75%) and least circulating *kfuC* (62.5%). Neither of Ybt synthesis gene was present in all isolates of ST43 and ranged between 50%-75%. Gene *iutA* was present in all isolates, while genes *iucABCD* ranged between 62.5-75%.

In ST16 (*n* = 7), a combination of K81 and OL101 was detected commonly. All the ST16 genomes had all *mrkABCDFHIJ* except one genome that lacked *mrkH* gene. Notably, all genomes had dual copy of *mrkA* and *mrkC*. Surprisingly, less than 30% of genomes had Ybt genes except *irp1* that was completely absent in ST16 genomes. Aerobactin transport gene *iutA* was detected in all isolates except one, while aerobactin synthesis genes were missing in all genomes. Every isolate had the K1 and O1 types in the ST23 (*n* = 6) genomes. It's concerning that every ST23 isolate carried the *rmpA* and *rmpA2*genes. The detection range for all *mrkABCDFHIJ* genes was 66.66%-83.33%, except for *mrkH* (16.66%). Gene *kfuA* was most frequent followed by *kfuB* and *kfuC*. In Ybt genes, *fyuA* was detected in all ST23 genomes, however others detected in range of 83.33%-100% except *ybtQ* (66.66%). Genes *iroBCDN* also detected in all isolates except one genome that lacked both *iroC* and *iroD*. Gene *iutA* alongwith *iucABCD* detected in all genomes. Interestingly some other less common virulence genes such as *all, fdrA, gcl, glx, ybb*, and *ylb* detected in all ST23 genomes, whereas gene *clb*, *mce, arc*, and *hyi* also detected in ST23.

Genome of ST196 (*n* = 5), all were belonged to K46 and O3/O3a type. Genes *mrkABDI* were detected in all isolates, while *mrkJ* was seen in 80% of isolates, interestingly none of the ST196 genomes had *mrkCFH*. Interestingly, neither genome had *kfuA*, and *kfuB*. only *kfuC* gene was detected in all isolates. In genome of ST101 (*n* = 4), the most common combination was K17 and O1. Except *mrkA* and mrkB, rest of the *mrk* genes were detected in all ST101 genomes. *kfuA* was detected in all isolates while *kfuB* and *kfuC* was seen in 50% of isolates. In Ybt genes, *fyuA*, and *ybtASTX* were detected in all isolates followed by *irp1*, *irp2*, and *ybtEPQ* in 75% genomes, and the least frequent *ybtU* in 50% genomes of ST101. All *mrkA*, *mrkC* and *ybtA* genes were detected in two copies across the genome of ST101.

5.3.3 String Test

A string test was conducted to investigate the mucoid phenotype. The formation of a viscous string of over 5mm in length was seen as a positive event. **Figure 5.7** illustrates that the isolate M20 and M58 exhibited a positive result for the string test, while the other isolates yielded negative results.

Figure 5.7 String test. Two positive isolates M20 and M58, which exhibited a string of more than 5 millimeters in length on a 5% Sheep blood agar plate.

5.3.4 Capsule staining and capsule size determination

Capsules from various *K. pneumoniae* isolates were examined under a microscope at a magnification of 100X. It was noticed that all isolates exhibited capsules in their surroundings as shown in **Figure 5.8**.

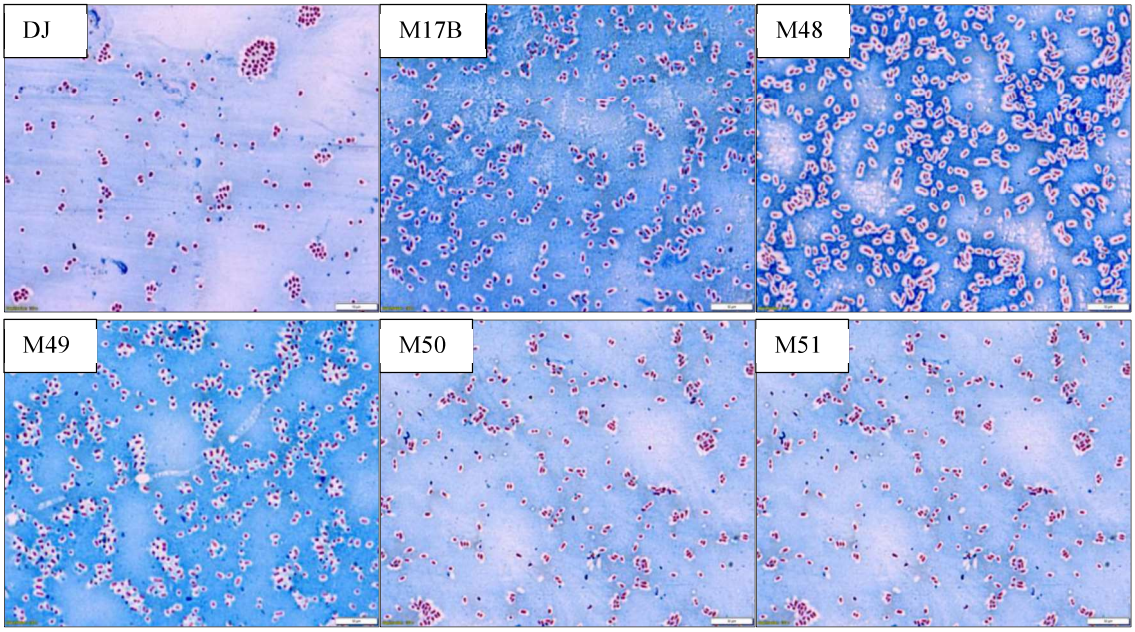

Figure 5.8 Capsule staining. Six representative isolates (DJ, M17B, M48, M49, M50, and M51) with a white-colored capsule layer around the isolates.

Size of the capsules was estimated for a minimum of 100 bacteria using Image J software. The graphical representation of **Figure 5.9** illustrates the average size of capsules for each isolate. M48 and M49, two isolates from the K64 subtype, were found to be almost identical in size, but DJ, the third isolate, had a lower capsule size. A similar finding was seen for the isolates connected to K51, indicating that isolates M50 and M51 had larger capsular sizes than isolate M57. K2-type isolate M17B had a moderately sized capsule; surprisingly, among the isolates, string positive strain M58 had the second-smallest capsule size, just below DJ.

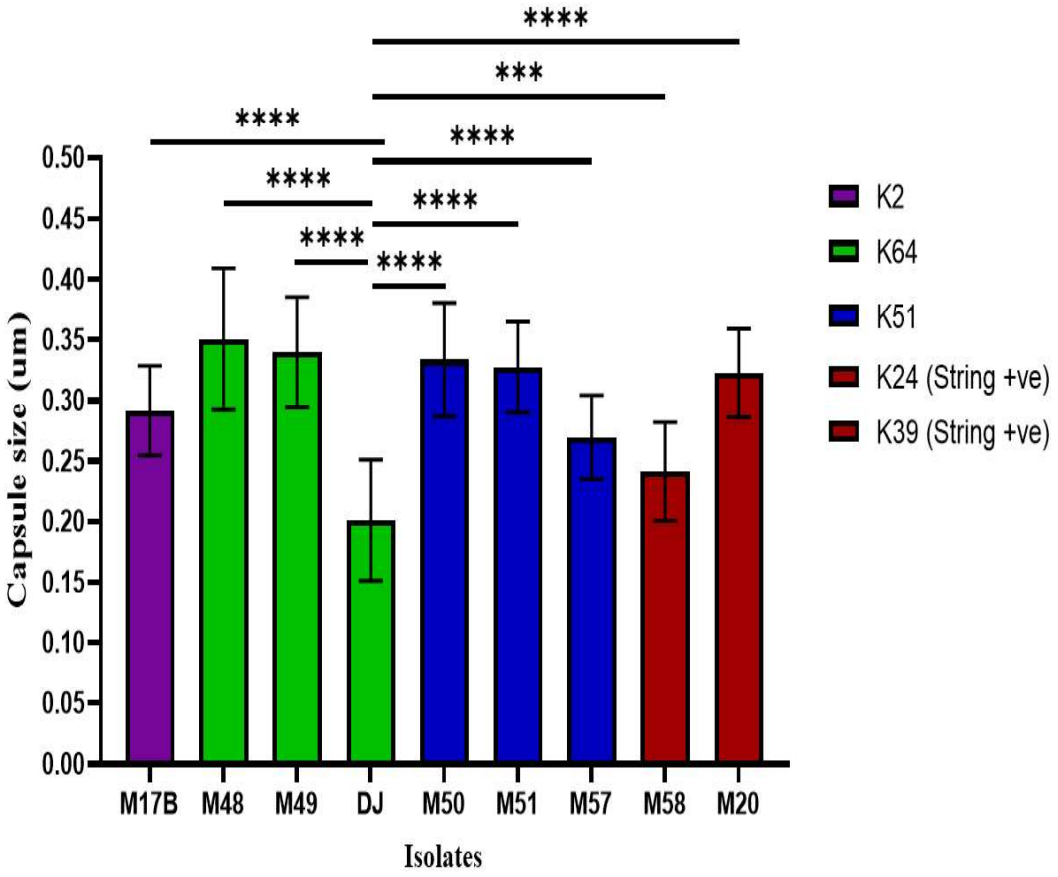

Figure 5.9 Graphical depiction of the size (in µm) of chosen isolates' capsules. The K-serotype of each isolate is shown by bars of orange, green, and blue colors, corresponding to K2, K64, and K51, respectively. The graph's colour bar indicates isolates that are positive for the string with K24. The statistical analysis was conducted using GraphPad Prism 8. Statistical analysis was performed using GraphPad Prism 8. *p<0.05; **p<0.01, ***p<0.001, ****p<0.0001.

5.3.5 Hypermucoviscosity assay

In the mucoviscosity experiment shown in **Figure 5.10**, it was found that the isolate M17B exhibited the lowest amount of mucoviscosity, while the isolate M58 shown the highest level of mucoviscosity. Within the various K-serotypes, it was observed that two isolates, DJ and M49, from the K64 group had a greater degree of mucoviscosity compared to isolate M48, which shared the same K-type. A same finding was seen in relation to isolates linked with K51, wherein isolates M51 and M57 exhibited a higher degree of mucoviscosity compared to M50.

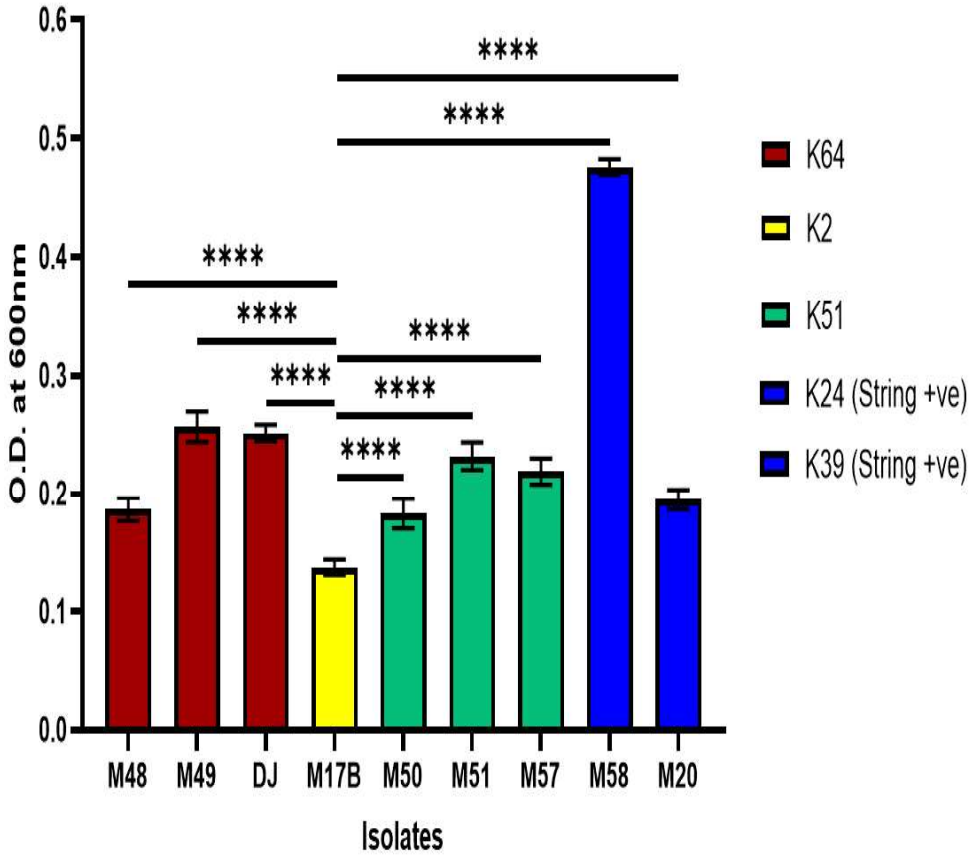

Figure 5.10 Graphical depiction of varying amounts of mucoviscosity seen in selected isolates. The K-type linked with each isolate is shown by the different colors, where orange, blue, and green correspond to K64, K2, and K51, respectively. Green color indicates isolates with string positive phenotype. Statistical analysis was performed using GraphPad Prism 8. *p<0.05; **p<0.01, ***p<0.001, ****p<0.0001.

5.3.6 Phagocytosis assay

The basis of our investigation of phagocytosis lies in the examination of the fluctuations in fluorescence intensity shown by neutrophils, as seen in **Figure 5.11 (A), (B), and (C)**. The distribution of cells depending on their fluorescence intensity that have effectively seen via the use of histograms. The primary variable of focus is the mean fluorescence (MFL) shown by all neutrophils. According to the investigation, it was noted that isolate M51 and M49 exhibited the greatest susceptibility to phagocytosis, whilst isolate DJ had the lowest susceptibility to phagocytosis.

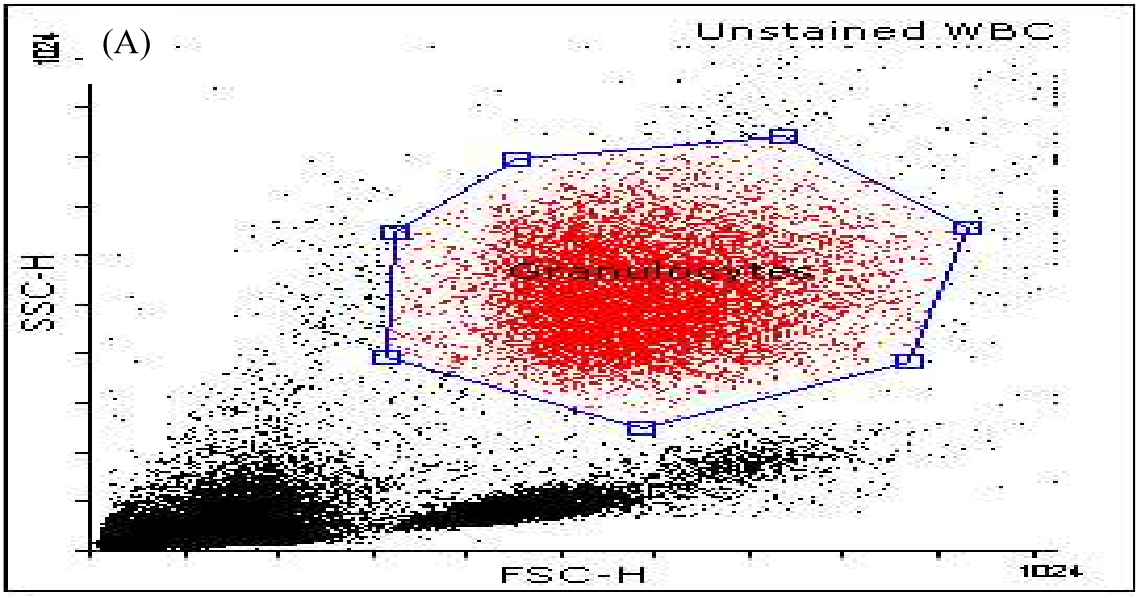

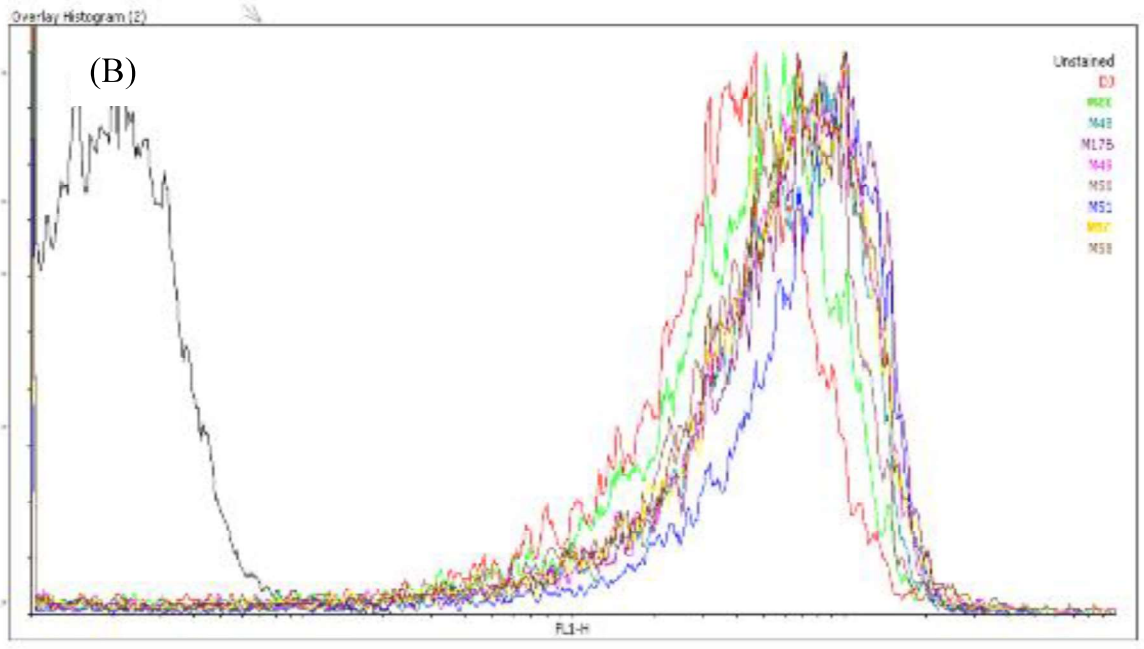

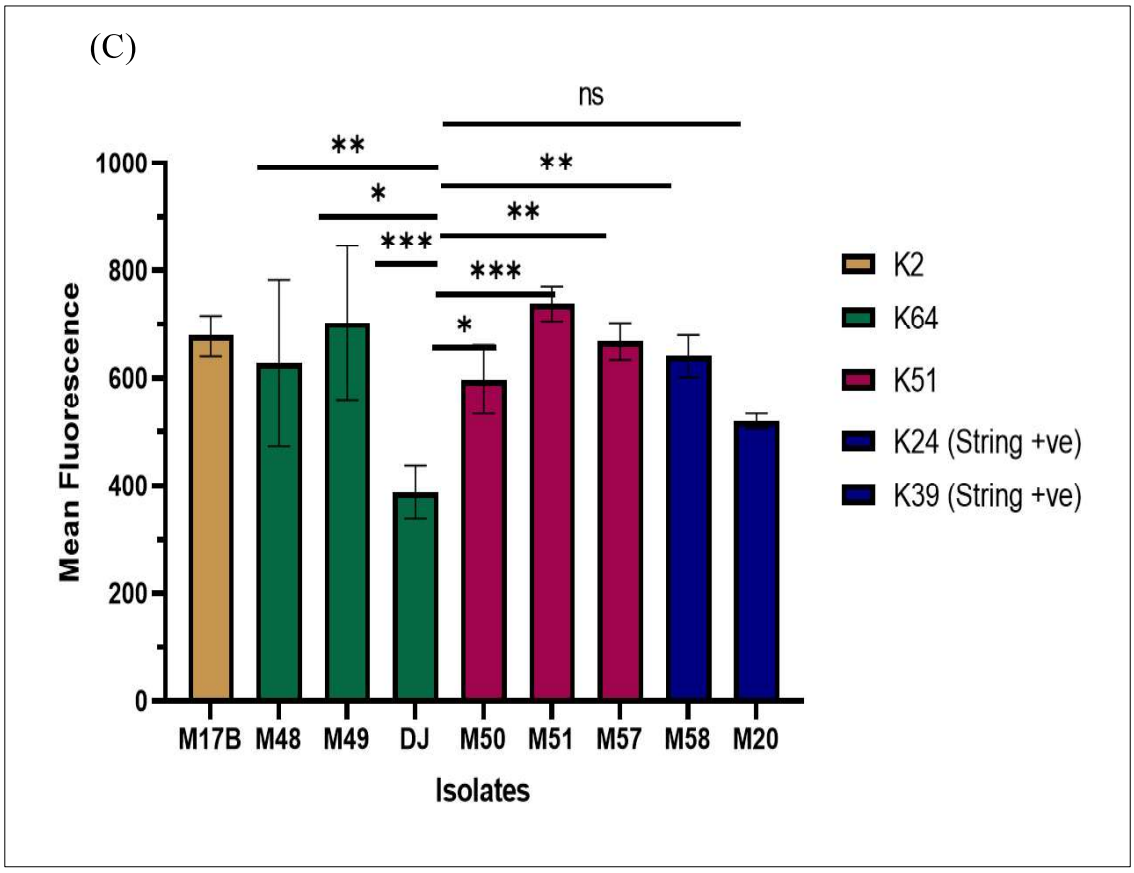

Figure 5.11 FACS data analysis. Figure 5.11(A) displays the overall population of unstained white blood cells (WBCs), with a focus on granulocytes for the purpose of analysis and data evaluation. **Figure 5.11(B)** displays the overlay histogram of fluorescence intensity, indicating that Isolate DJ exhibited the least sensitivity to phagocytosis, whereas isolates M51 and M49 had the greatest vulnerability to phagocytosis. **Figure 5.11(C)** displays the average fluorescence of each isolate. In contrast to the least sensitive isolate DJ, all other isolates exhibited higher levels of fluorescence, and this difference was statistically significant. Statistical analysis was performed using GraphPad Prism 8. *$p<0.05$; **$p<0.01$, ***$p<0.001$, ****$p<0.0001$

5.3.7 Serum Killing Assay

The isolates M17B, M49, M57, and M58 were all serum sensitive, apart from isolate M57, all had the O2a-serotype in common. However, M48 and DJ were both intermediately sensitive and belonged to the O1 + K64 and O2a + K64 types, respectively. Serum killing resistance was

identified in M50 and M51, which were both notable instances of the O1 + K51-type and the most prevalent in Indian *K. pneumoniae* genomes. The Representative images of serum susceptible, intermediate, and resistant were shown in **Figure 5.12.**

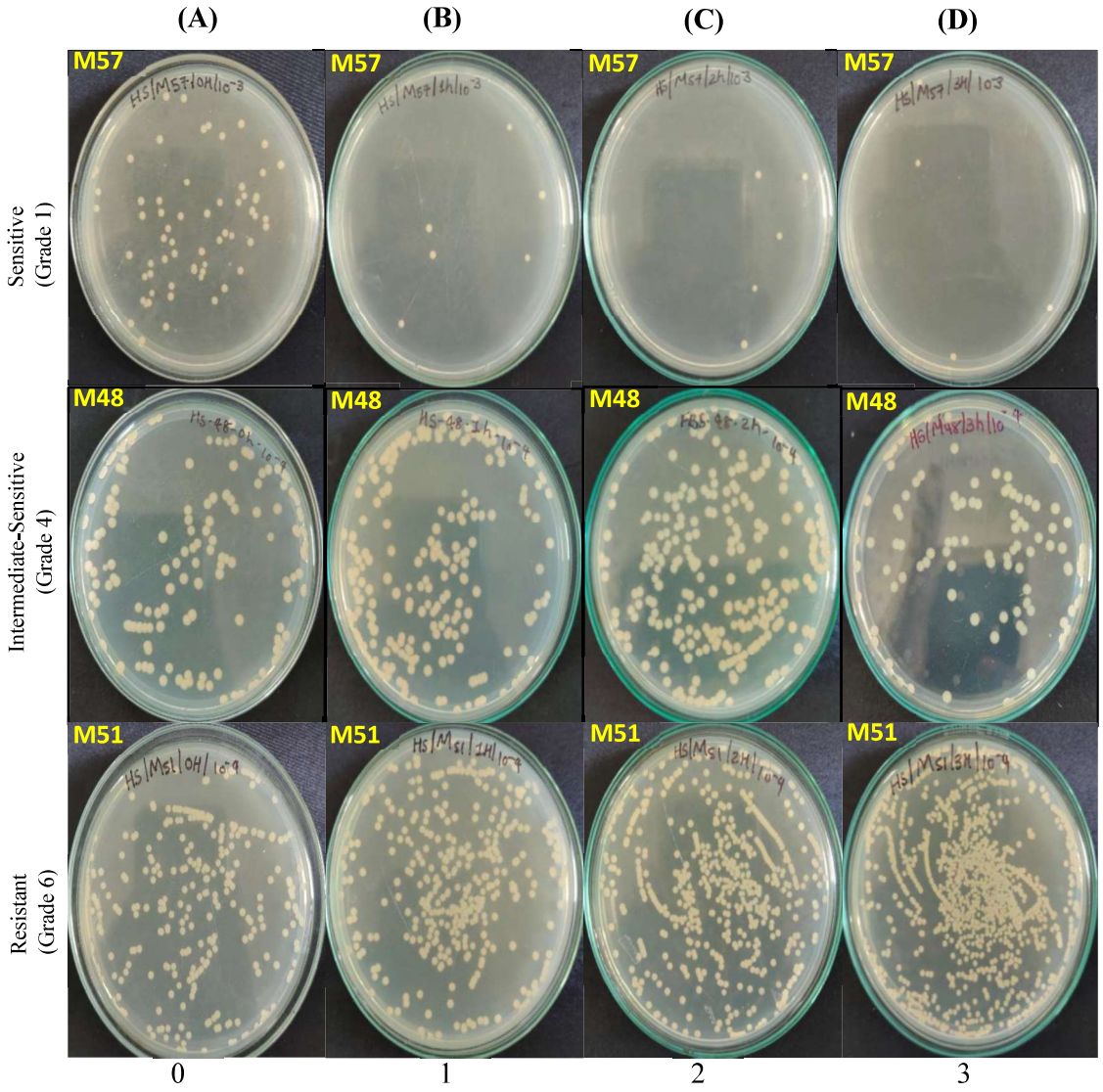

Figure 5.12 Serum killing assay results for the representative isolates M57, M48, and M51. Presented here are typical isolates from each of the three categories: M57, which is susceptible to serum; M48, which has intermediate sensitivity; and M51, which is resistant. The culture plate identified as a, b, c, and d correspond to the incubation periods of isolates with serum at 0 hours, 1 hour, 2 hours, and 3 hours, respectively.

To summarize the relationship between genotypic and phenotypic data of virulence, The combination of ST231 (K51 + O1) had the greatest occurrence among isolates, followed by ST2096 (K64 + O1), ST14 (K2 + O1), and ST147 with two distinct combinations: K64 + O2a and K10 + O3/O3a. Additionally, these isolates included a substantial number of virulence genes. In order to assess the virulence potential of these combinations, a set of representative isolates were created and thoroughly examined for their virulent characteristics. No link was seen between capsule size, hypermucoviscosity, and string test with significant virulence features. However, phenotypic examinations have shown that in 50% of the tested isolates, the deadly combination of K51 + O1 showed resistance to serum and was also less susceptible to phagocytosis. However, when examined individually, a significant correlation between the O1 serotype and resistance to serum was seen. This is alarming since the O1 serotype was the most common O-type, including almost 60% of the *K. pneumoniae* genomes identified in India. The K51 + O1 combination was the most common among ST231 isolates. These isolates included many genes in their genome, including the *iutA* and *iucABCD* gene clusters, which are responsible for the production of aerobactin. This is considered one of the markers of a hypervirulent strain. In **Chapter 4**, it was previously shown that the majority of ST231 isolates belong to the XDR and PDR categories and have one or more genes (*bla*OXA-48-like and *bla*NDM) that confer resistance to carbapenem drugs. Additionally, a small number of ST231 isolates have also exhibited resistance to colistin.

Moreover, upon closer examination of the data obtained from lab isolates, it becomes apparent that both ST231 and ST2096 exhibit a higher quantity of genes associated with antimicrobial resistance, such as carbapenemases, and virulence, such as aerobactin as shown in **Figure 5.13.** Additionally, their phenotypic characteristics indicate that they fall into the categories of extensively drug-resistant and multidrug-resistant in terms of drug resistance patterns. Regarding their pathogenicity, they belonged to O1 serotype and exhibited resistance to serum and a slightly reduced susceptibility to phagocytosis by neutrophils. This indicates that the clones of ST231 and ST2096 convergent strains, which is alarming. Further, these strains used ICEKp5 as a common carrier to transmit the *ybt14* variants of *ybt* gene cluster, consequently transforming normal strains into pathogenic strains. Therefore, it is imperative to consistently monitor and undertake more studies on these two clones.

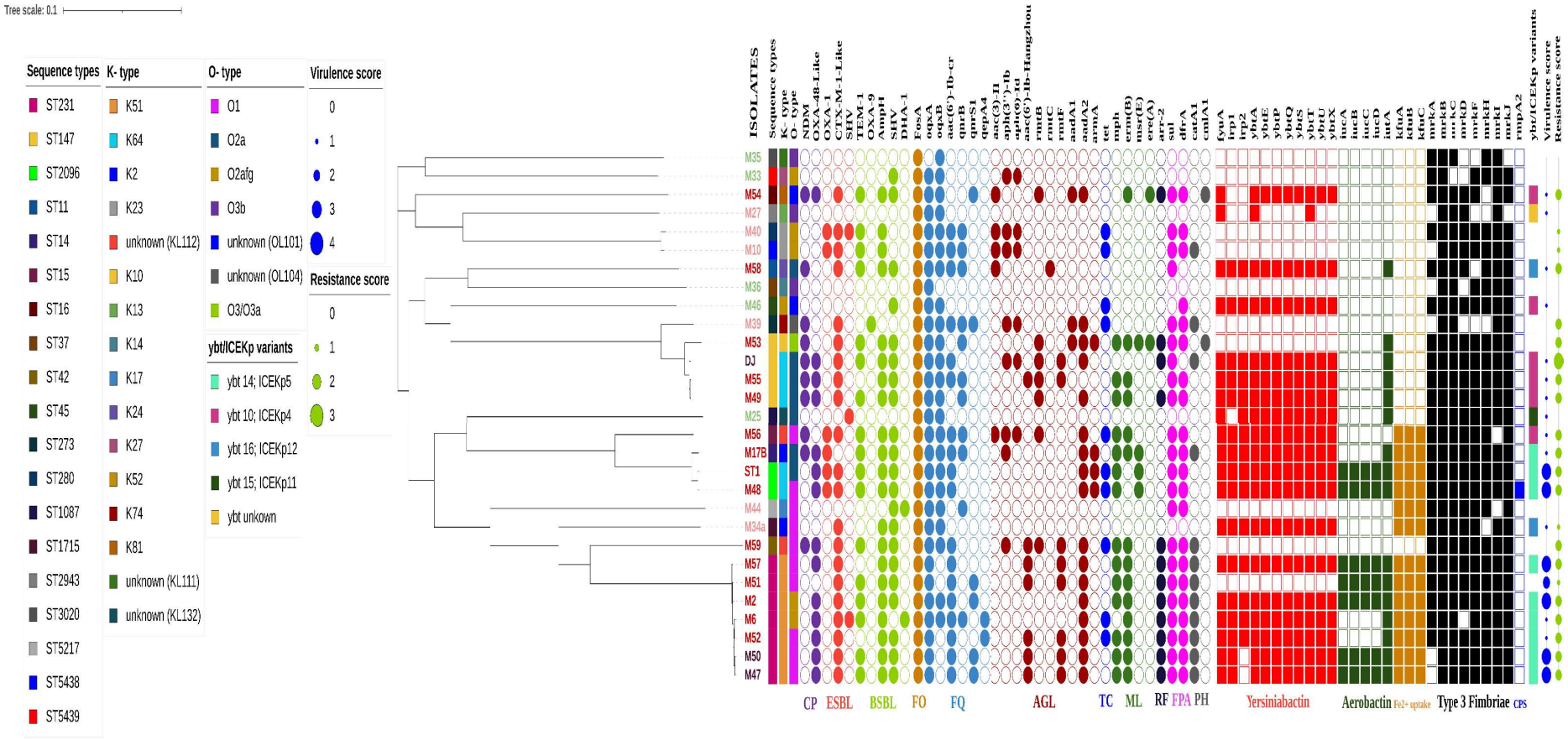

Figure 5.13 Overall genetic makeup of laboratory isolates (*n* = 29). The isolates listed in various colors show their drug susceptibility profile: green for **susceptible**, light red for **MDR**, red for **XDR**, and dark red for **PDR.** In the resistance and virulence score, a bigger circle size signifies a higher resistance score and virulence, which in turn suggests a greater number of genes for AMR and virulence present in the genome. Circle and square filled with different colours indicates presence of AMR and virulence genes respectively, while blank indicates absence of genes.

(Abbreviations: CP- carbapenems, **ESBL-** extended spectrum beta-lactams, **BSBL-** broad spectrum beta-lactams, **FO-** fosfomycin, **FQ-** fluoroquinolones, **AGL-** aminoglycosides, **TC-** tetracyclines, **ML-** macrolides, **RF-** rifampin, **FPA-** folate pathway antagonist, **PH-** phenicols; **CPS-** capsular polysachharides)

5.3.8 Qualitative detection of Siderophore:

All isolates tested positive for siderophore in the qualitative detection assay. They exhibited a distinct yellowish zone surrounding the colony against a dark green/blue background, indicating the synthesis of siderophores by the bacterial isolates on CAS agar medium as shown in **Figure 5.14 (A), (B), and (C).**

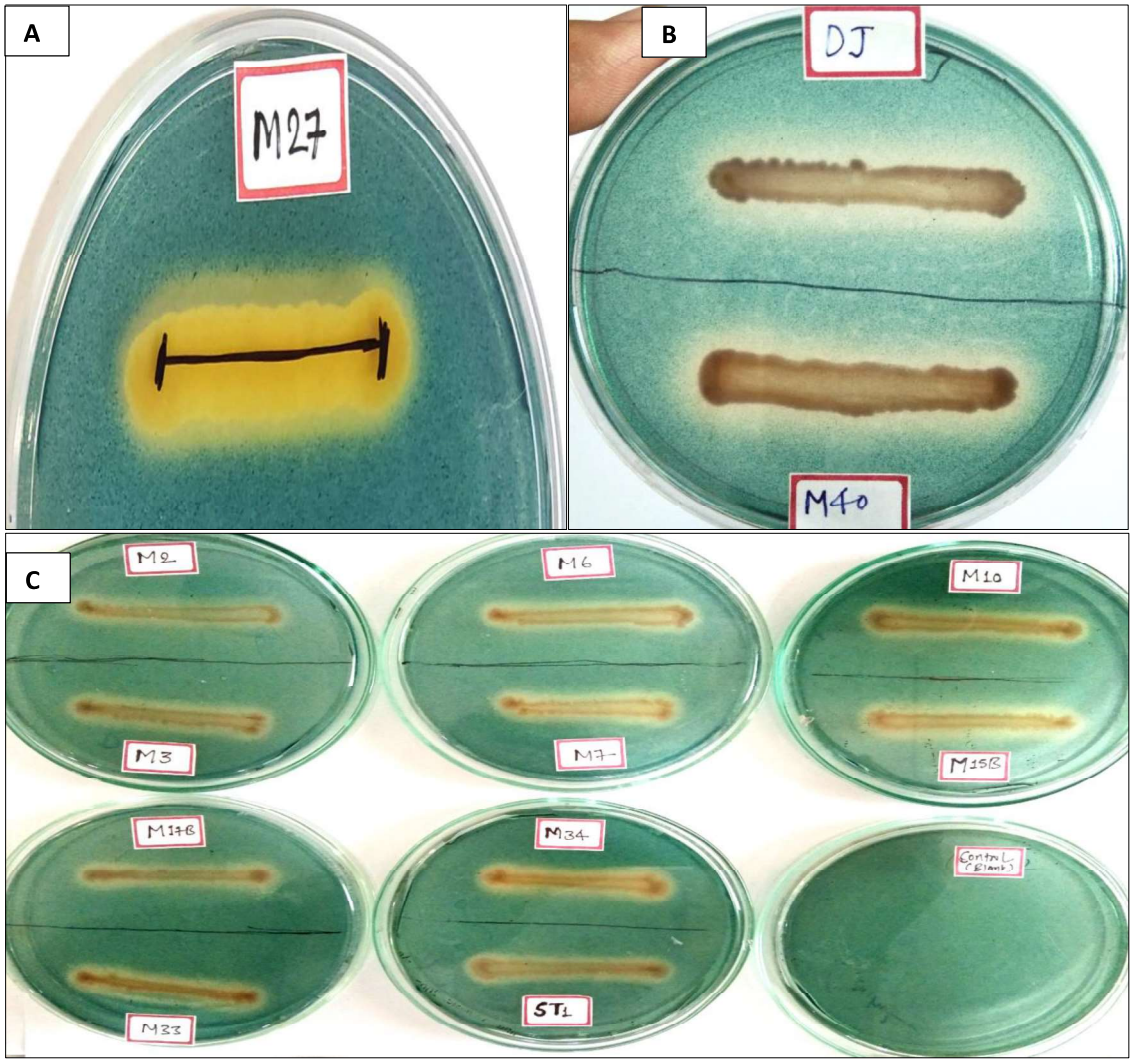

Figure 5.14 Representative pictures of isolates showing production of siderophore on CAS agar medium. All isolates shown in Figure 5.14(A), (B), and (C) exhibited the production of siderophore, which was seen as yellowish color surrounding the bacterial colonies against the greenish background. Figure 5.14(C) included a blank plate to perform a sterility check as a negative control.

5.3.9 Quantitative detection of siderophore

During the quantification of siderophores using a modified microtiter plate approach, we detected variations in the amount of siderophore synthesis. Isolate M57 had the greatest siderophore production with greater than 20%, followed by M53, M2, M54, and M59, all of which had a siderophore production percentage in range of 15%-20%. However, the isolates M6, M10, M25, M27, M34a, M35, M39, M46, M50, M56, and ST1 exhibited low siderophore production, with less than 5% as shown in **Figure 5.15**.

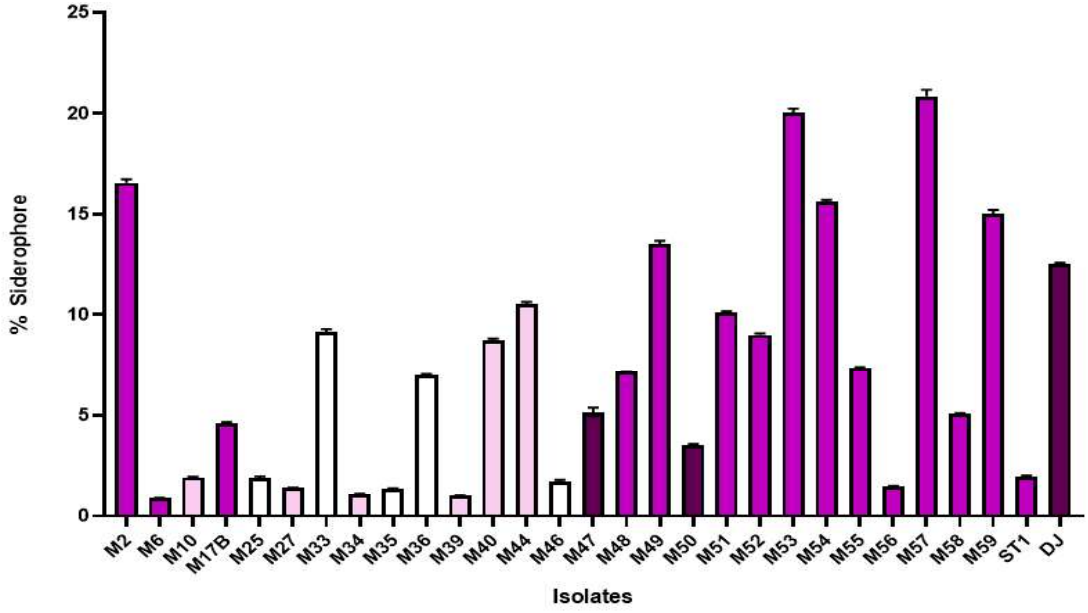

Figure 5.15 Percentage of siderophore synthesis by lab isolates (*n* = 23). Isolate M57 had the greatest production, exceeding 20%. It was followed by M53 and M2, while M6 had the lowest output among the isolates. The bars' color represents their drug resistance category, with white indicating susceptibility to drugs, pale pink indicating multidrug-resistance, dark pink indicating extensively-drug resistant, and chocolate brown indicating pandrug-resistance.

5.3.10 Study on effect of iron and iron chelator and antibiotics on %siderophore production

This study investigated the impact of iron and a chelator (DIP) on the growth of selected isolates and their capacity of siderophore production as shown in **Figure 5.16**. Six distinct isolates M10 (MDR,), M33 (Susceptible), M48 (XDR), M50 (PDR), M51 (XDR), and M52 (XDR) of *K. pneumoniae* based on their resistance and genomics profile for siderophore genes M10 (*ent*+, *ybt*-, *iuc*-), M33 (*ent*+, *ybt*-, *iuc*-), M48 (*ent*+, *ybt*+, *iuc*+) M50 (*ent*+, *ybt*+, *iuc*+), M51 (*en*t+, *ybt*-, *iuc*+), and M52 (*ent*+, *ybt*+, *iuc*-) as shown in **Figure 5.13**. Since all isolates had genes for enterobactin, they are now no longer considered virulence genes as per the virulence database at PasteurMLST, available at https://bigsdb.pasteur.fr/klebsiella/, so it was not mentioned in **Figure 5.13.** All the isolates exhibited an optical density (OD) at 600 between 0.2 and 0.3 when cultured on LB medium without any additional supplements. The formation of siderophore was found in all the isolates, with levels ranging up to 10%. All isolates exhibited robust growth compared to the control in the presence of iron at all three doses (100 uM, 50 uM, and 25 uM). However, no siderophore synthesis was seen in any of the isolates with the presence of iron.

However, when an iron chelator (DIP) was present, it was shown that the growth of all tested isolates irrespective of their genetic makeup for siderophore genes were substantially inhibited as the concentration of DIP increased. Nevertheless, there remained uncertainty over the ability to produce siderophores in the presence of DIP. A consistent pattern was seen isolate M10 and M48, where an increase in the concentration of DIP resulted in a corresponding rise in siderophore synthesis. The generation of siderophore was markedly increased by about 30% in M48 and 20% in M10 compared to the control (<10% in both the isolates). In contrast, isolate M51 and M52 had a pattern identical to M10 and M48, but the total production of siderophores was either equivalent to or less than the control (about 10%) throughout all three dosages of DIP. The generation of siderophore reached its maximal level in isolate M33 and M50 when the concentration of DIP was increased to 400 uM. In M33, the level of siderophore synthesis reached its highest point when exposed to 400 uM of DIP, which was almost equivalent to the control. However, in M50, the maximum siderophore production with 400 uM of DIP was notably higher than the control.

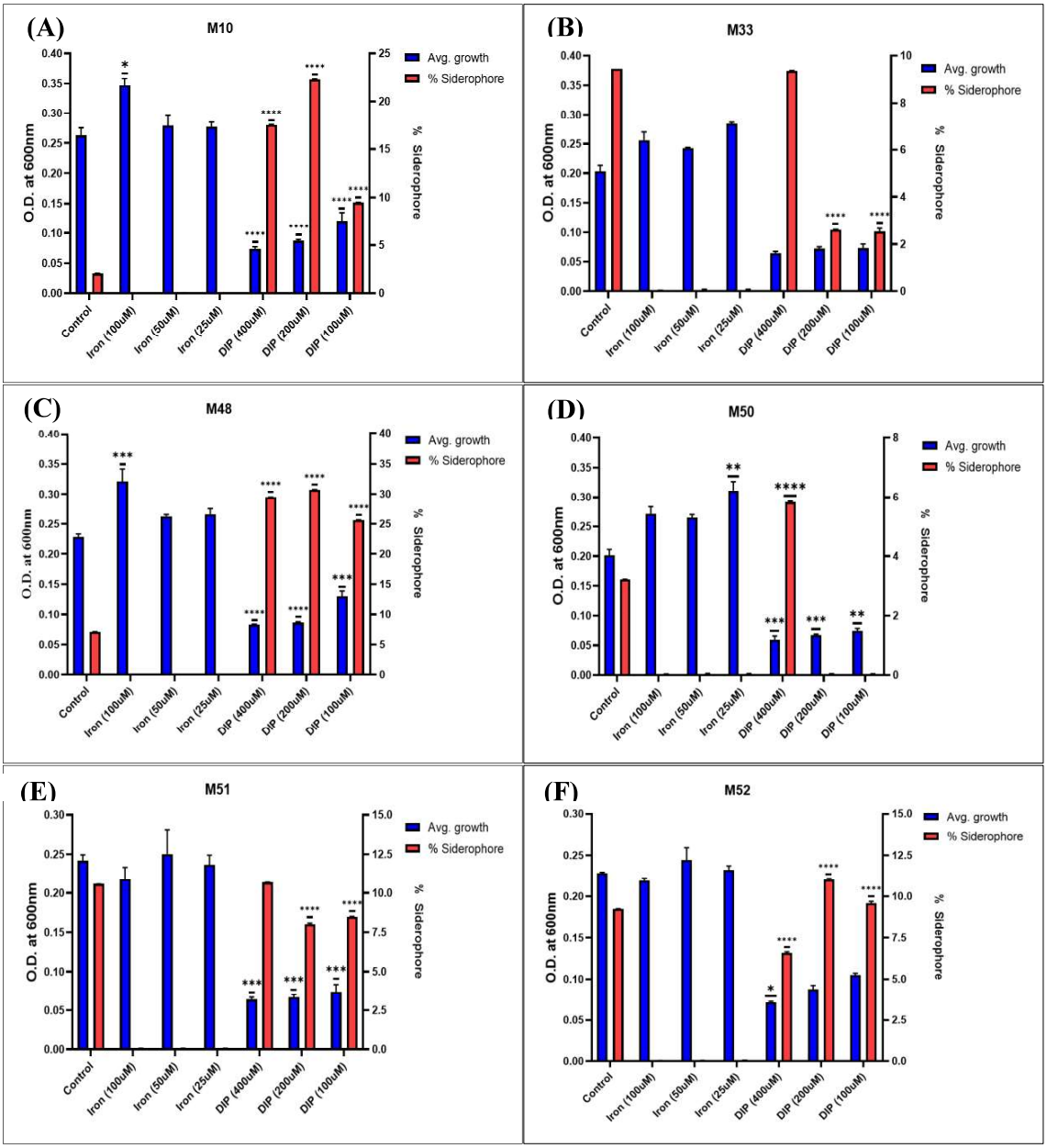

Figure 5.16 Growth and the percentage of siderophore formation in presence of iron and DIP. Selected isolates (A) M10, (B) M33, (C) M48, (D) M50, (E) M51, and (F) M52 exposed to iron and DIP (an iron chelator) at three different concentrations: iron (100 uM, 50 uM, and 25 uM) and DIP (400 uM, 200 uM, and 100 uM). The purple bars indicate the average growth of isolates, and the red bars indicate the % siderophore production of isolates. Statistical analysis was conducted using a one-way ANOVA with GraphPrism 8.4.2 employing Dunnett's multiple comparisons test, were each sample was compared with the control group. *p<0.05; **p<0.01; ***p<0.001; ****p<0.0001; no significance p>0.05.

However, in presence of antibiotics (ampicillin, ciprofloxacin, and colistin), isolates M48, M50, and M52 exhibited excellent growth even in the presence of ampicillin at all tested

concentrations (5 ug/ml to 40 ug/ml) as shown in **Figure 5.17**. While an increase in the concentration of ampicillin resulted in decrease in growth reported in M10, M33, and M51. More precisely, isolate M33 showed limited growth at all doses of ampicillin, while M10 and M51 exhibited significant growth restriction at concentrations of 20 ug/ml and 40 ug/ml. Regarding siderophore production capabilities, isolates M10, M48, and M52 consistently do not produce siderophore when exposed to all tested doses of ampicillin. In isolate M33, the synthesis of siderophore decreased as the concentration of the ampicillin antibiotic increased. In isolate M50, only at a concentration of 40 ug/ml was the production of siderophore detected in a very significant amount, which was more than the control. Remarkably, in M51, the proportion of siderophore rose as the concentration of ampicillin increased, while the generation of siderophore was lower than the control. When ciprofloxacin was examined at concentrations ranging from 1.25 ug/ml to 10 ug/ml, no significant decrease in growth was seen in isolates, except for M10 and M33. In the case of isolate M10, a noticeable decrease in growth was detected at concentrations of 5 ug/ml and 10 ug/ml. However, in the case of isolate M33, a substantial reduction in growth was observed at all four concentrations. Remarkably, the production of siderophore in all isolates exhibited a direct correlation with the rising concentrations of ciprofloxacin drug. The presence of siderophore was observed at a concentration of 10 ug/ml of ciprofloxacin in isolate M33, reaching up to 50% production. Except for M10, all other samples exhibited siderophore production over 20% at a concentration of 10 ug/ml of ciprofloxacin. Except for isolates M48 and M50, a considerable decrease in growth was seen in the presence of colistin. However, in isolate M10, the growth was not suppressed at lower doses (0.31 ug/ml and 0.62 ug/ml) of the medication, but it was significantly decreased at higher concentrations (1.25 ug/ml and 2.5 ug/ml) of the medicines. Differences in siderophore production were noted across isolates in the presence of colistin. Specifically, isolates M48, M51, and M52 did not produce siderophore at any of the four tested doses, except for isolate M51 and M52 which showed production at a dosage of 0.31 ug/ml. However, in other isolates, M10 and M33 exhibited a considerably increased production of siderophore compared to the control at lower concentrations (0.31 ug/ml and 0.62 ug/ml), although this production decreased at higher drug doses (1.25 ug/ml and 2.5ug/ml). Unlike M10 and M33, isolate M50 exhibited a contrasting trend, with siderophore synthesis rising in tandem with higher doses of colistin medication. And the highest production of siderophore, at about 30%, was seen at a drug concentration of 2.5 ug/ml. Conversely, the lowest production, around 10%, was discovered at a concentration of 0.31 ug/ml of colistin. However, in both cases, the amount of siderophore was more than that of the control.

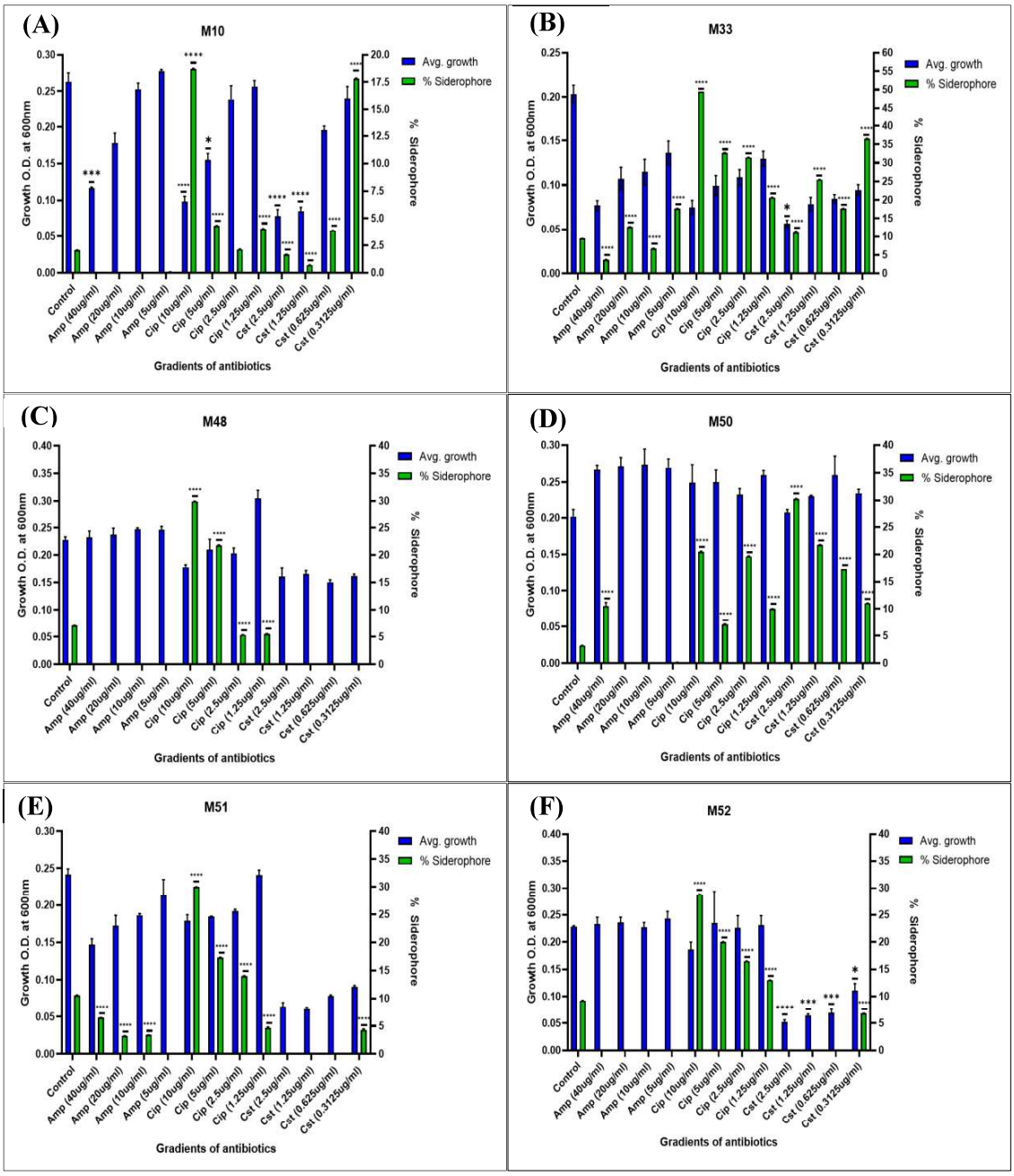

Figure 5.17 Growth and percentage of siderophore production in presence of antibiotics. Selected isolates (A) M10, (B) M33, (C) M48, (D) M50, (E) M51, and (F) M52 exposed to three different antibiotics at four different concentrations. The antibiotics used were ampicillin (40 ug/ml, 20 ug/ml, 10 ug/ml, and 5 ug/ml), ciprofloxacin (10 ug/ml, 5 ug/ml, 2.5 ug/ml, and 1.25 ug/ml), and colistin (2.5 ug/ml, 1.25 ug/ml, 0.625 ug/ml, and 0.31 ug/ml). The blue bars indicate the average growth, and the green bars indicate the % siderophore production. Statistical analysis was conducted using a one-way ANOVA with GraphPrism 8.4.2 employing Dunnett's multiple comparisons test, were each sample was compared with the control group. *p<0.05; **p<0.01; ***p<0.001; ****p<0.0001; no significance p>0.05.

5.4 Discussion

The research found a total of 93 distinct sequence types, indicating the wide range of variety and rapid evolution in *K. pneumoniae* genomes as a result of mutations. Although not all sequence types provide a significant hazard in terms of virulence and antibiotic resistance, there are a few key and widespread STs that present serious challenges as a threat to public health. These STs should be continuously monitored. Given the aforementioned factors, this study was conducted to ascertain the frequency of noteworthy STs, K-type, and O-type, together with their phenotypic traits. The research used a restricted number of representative isolates to collect fundamental data. ST231 was identified as the most common sequence type, as previously reported by other studies from India (Shankar et al., 2020; Nagaraj et al., 2021; Sundaresan et al., 2022). However, there has been a shift in trends with ST14 emerging as the second most frequent sequence type, exceeding the previously second most common ST147 (Shukla, Desai, et al., 2023). With the exception of ST231 and ST14, the prevalence of all other STs was below 10%. This research identified 43 out of the more than 140 known K-types circulating in the Indian genomes of *K. pneumoniae*, as well as a total of 13 different O-types. Fortunately, the occurrence of well recognized highly infectious K-types like K1 and K2 was less frequent, whereas K51 and K64 were the most prevalent in Indian *K. pneumoniae* genomes. Collectively, K51 and K64 accounted for around 45%. Another seroepidemiology investigation examined Taiwanese bacteremia patients' *K. pneumoniae* isolates over 20 years. In 48.5% of isolates, the top five capsular polysaccharide serotypes (K1, K2, K20, K54, and K62) were consistently frequent (Liao et al., 2022; Tsai et al., 2023). The capsular serotypes K1, K2, K47, and K64 are frequently linked to increased virulence in *K. pneumoniae*, known as hypervirulent strains. Additionally, isolates belonging to the K64 and K47 serotypes are often associated with resistance to carbapenem, making them hypervirulent carbapenem-resistant strains. The high occurrence of these isolates has presented substantial risks to human health, and there are now no suitable treatments available to combat them (Z. Wang et al., 2022). To develop effective control methods, such as vaccinations, for mitigating the burden of outbreaks arising from hypervirulent and carbapenem-resistant *K. pneumoniae* strains, it is crucial to comprehend the features and problems connected with serotype K64. The study's emphasis on K64 underscores the need of targeting certain serotypes to enhance treatment results and public health interventions.

The distribution of O-serotypes among Indian *K. pneumoniae* isolates showed limited variety, with O1 accounting for over 60% of the isolates, while the other serotypes were each below

10%. Two distinct combinations of ST231 were identified, with ST231 (K51 + O1) being the predominant variant. This particular variant was also the most common among all STs, while a few isolates exhibited ST231 (K51 + O2afg). The prevalence of type 3 fimbriae-related genes *mrkABCDFHIJ* was highest among all identified virulence factors, with roughly 93% of isolates possessing these genes. In general, the presence of genes associated with type 3 fimbriae, yersiniabactin, and salmochelin was seen in the ST231 strain. Nevertheless, the aerobactin gene was found in only around 50% of cases. However, there is a shortage of reports indicating the existence of isolates generating the K51 capsular type in worldwide data. However, only a small number of reports have shown the existence of the ST16-K51 isolate (Hallal Ferreira Raro et al., 2023). Although there is a dearth of data especially on K51, as described in the literature, this investigation will contribute to our understanding of the virulence characteristics of the K51 capsular type. Also, in a previous study conducted by (Sundaresan et al., 2022) in India, the prevalence of K51 was observed among 153 *K. pneumoniae* isolates.

The second most common ST14 showed three combinations: ST14 with (K2 + O1) and (K2 + O3/O3a) were the main combinations, and (K64 + O1) was a less common type of combination that showed a gene cluster linked to type 3 fimbriae and yersiniabactin. Unfortunately, we found that both gene clusters were present in 100% of cases for ST14 (K2 + O3/O3a) and the type 3 fimbriae gene cluster in ST14 (K2 + O1) and ST14 (K64 + O1). Fortunately, the gene clusters responsible to produce aerobactin and salmochelin, which are the second-most common types of ST, were not present. Out of the two main combinations of ST147 with (K64 + O2a) and (K10 + O3/O3a), only two kinds of gene clusters for tytpe 3 fimbriae and yersiniabactin were found. Among these, ST147 (K64 + O2a) exhibited a higher prevalence of these two gene clusters. The genes that function as activators of capsule biosynthesis, such as *rmpA*, were found to be present in 100% of the ST23 (K1 + O1) strains. On the other hand, *rmpA2* was seen in ST2096 (K64 + O1), ST11 (K24 + O2a), and ST43 (K30 + O1). In recent research from Japan, it was found that there was a distinct pattern seen, with the exception of ST23. Multilocus sequence typing analysis showed that there were several sequence types among the rmpA-positive isolates. The most common sequence type was ST23/K1, followed by other sequence types such as ST412/non-K1/K2, ST86/K2, and ST268/non-K1/K2. The presence of genetic variety among rmpA-positive *K. pneumoniae* strains indicates that there is genetic variability (Kikuchi et al., 2023). Also, contrary to our results, a separate study revealed that ST147 was the primary carrier of the *rmpA* and *rmpA2* genes in *K. pneumoniae* from the

United Kingdom (J. F. Turton et al., 2024). Other studies also described the prevalence of *rmpA/2* genes in ST23 (Khrulnova et al., 2022), in ST15 from China (Tian et al., 2022). Notably, all four combinations in our study shared the O1 serotype, indicating that the O1 serotype may have a crucial role in hyper capsule biosynthesis and pathogenicity. However, it is not necessary for all instances of the O1 serotype to must possess the *rmpA* and *rmpA2* genes as found in ST231 and ST14. Another research conducted in India revealed that KL51:O1v2, KL17:O1v1, and KL64:O2v1 were the most often found capsular serotypes among the isolates of *K. pneumoniae*, with KL64 being the most common (Moses et al., 2024). Multiple investigations have consistently shown a strong correlation between the presence of K64 and ST11 in the genetic makeup of hvKp isolates. This indicates that strains with this particular capsule serotype have a unique genetic background (Sanikhani et al., 2021; Z. Wang et al., 2022). The research also observed a higher occurrence of capsule type K64 across pathogenic *K. pneumoniae* isolates, especially in instances of meningitis and sepsis. These findings indicate that K64 is linked to invasive infections acquired within the community in Vietnam (Vu Thi Ngoc et al., 2021).

Certain isolates belonging to the major sequence types ST43 (K30 + O1) and ST395 (K66 + O1) exhibited a deficiency in type 3 fimbraie genes. In addition, the less common ST196 (K46 and O3/O3a) did not possess these genes. Like our research, a few other investigations have shown that *K. pneumoniae* strains ST43 and ST395 do not possess the *mrk* genes that are responsible for producing type 3 fimbriae, notably *mrkABCDF* (Schurtz et al., 1994; Hornick et al., 1995; Y.-J. Huang et al., 2009). ST16 (K81 + OL101) and ST196 (K46 + O3/O3a) were discovered to be deficient in the gene clusters responsible for producing all three variants of siderophores. Similar to our findings, some studies have revealed that *Klebsiella* strains ST16 and ST196 lack the *iucA* and *iroB* genes, which are responsible for producing siderophores (M. M. C. Lam et al., 2018; Jassim et al., 2023). Another distinctive combination, ST23 (K1 + O1), was detected. This combination has all types of pathogenic genes identified in this investigation, with the exception of the *kvgAs* gene cluster. Fortunately, the number of these combinations among isolates was far lower. However, it is essential to consistently monitor and surveil certain sequence types and combinations to prevent significant epidemics. Multiple investigations have shown that the ST23 (K1) strain of *K. pneumoniae* in the research has many virulence genes, including those associated with capsule hyperproduction, bacteriocins, and siderophore biosynthesis (Morales-León et al., 2023). While it has been shown that only ST23 (K1 + O1) combinations had a greater number of virulence genes such

as *ybt, clb, iuc, rmpADC,* and *rmpA2*. In contrast, other ST23 (K57 O2) isolates have a lower number of virulence loci (Biedrzycka et al., 2022; M. M. C. Lam et al., 2023). The ST14 (K2 + O3/O3a) and ST23 (K1 + O1) strains pose a significant challenge and potential danger to public health in the future, according to the genomics data. This is due to the presence of virulence genes in all isolates or the discovery of a majority of genes in these combinations. In addition, the ST231 strain, which is the most common strain, has many types of virulent genes. Of particular concern is the presence of the aerobactin gene, which is a hallmark for hypervirulent strains and poses a significant danger to public health in India. Contrary to our findings, a West Indies study demonstrates that the genomic analysis successfully identified high-risk genotypes such as ST11, ST15, ST86, and ST307, as well as capsular serotypes KL17:O1v1, KL51:O1v2, and KL64:O2v1. However, K51 and O1 were the shared variables in both investigations (Pustam et al., 2023). Also, this specific combination of ST231 (K51 + O1) is less prevalent in America and Europe. However, in Asian continents, it has been identified in a few studies as a worrisome pathogen with elevated antimicrobial and pathogenicity capabilities (Spagnolo et al., 2014; Clegg & Murphy, 2016; X. Yang et al., 2022; Tsui et al., 2023).

In this research, also focused on analyzing the primary characteristics that contribute to the virulence of various combinations of typical *K. pneumoniae* isolates. These isolates were selected based on their sequence types, K-types, O-types, drug resistance profiles, genomic contents of virulent genes, and the presence of prophages in their genomes. The phenotypic study of capsule and lipopolysaccharides is centered on specific isolates (M17B, M20, M36, M48, M50, M51, M57, M49, M58, and DJ) that were categorized based on their K-type and O-type, along with their corresponding frequencies. Nevertheless, the isolates M58 (ST11, K24, O2a) and M20 (ST2943, K39, O3b) exhibited a positive string phenotype. These isolates belonged to less prevalent ST types, K-types, and O-types, and were specifically chosen for the phenotypic investigation.

In our study, the average size of the capsules ranged from 0.19um to 0.35um. The DJ and M58 isolates exhibited smaller capsule sizes, while the M48 and M49 isolates had bigger capsule sizes. Both intra- and inter-K-type *K. pneumoniae* isolates showed differences in capsule size. Out of the three isolates that belonged to K64 and K51, two of the K64 and K51 types had almost comparable sizes, while one of each K64 and K51 type showed lesser sizes. Differences in size were observed between two positively identified string isolates, with isolate M20 being somewhat bigger than isolate M58. There are certain reports showed that, the strains of

different types show variations in the thickness of their capsules, with virulent strains that are encapsulated having thicker capsules in comparison to avirulent strains (Meno & Amako, 1990). On the other hand, the amount of the capsule is affected by external elements like the presence of iron or the temperature, and these parameters are controlled by regulators that adjust the creation of the capsule (Haudiquet et al., 2024). Capsular swelling, which may be triggered by events such as therapy with anti-capsular serum or changes in environmental circumstances, can also affect the thickness of the capsule by causing it to enlarge and lose electron density. Of addition, the capsules of *K. pneumoniae* are composed of tightly packed fibers, with differences in organization and width noted across different strains (Amako et al., 1988). Moreover, the examination of genetic material has shown that the exchange of capsules is frequent among groups of genetically similar organisms, suggesting that changes in the thickness of the capsule may also be affected by genetic elements and the process of diversification (Wyres et al., 2016). Nevertheless, several publications assert that the pathogenicity of capsules is determined more by their kind rather than their thickness. The specific composition of the capsule in *K. pneumoniae* has a more significant role than its thickness in determining its ability to avoid being captured by Kupffer cells in the liver, which in turn affects its virulence and ability to survive (X. Huang et al., 2022). In another research, which indicates that the type of capsule in *K. pneumoniae*, namely the K1 capsule, is more important than its thickness for the spread of the bacteria in the circulation and the development of disease (Rendueles, 2020). In different study, it was also reported that the type of capsule in *K. pneumoniae* has a greater influence on fimbrial function, adhesion, and biofilm formation than its thickness (Schembri et al., 2005).

In the mucoviscosity experiment from this study, variations were noticed among the isolates, even within the same K-type. The study revealed that the M58 string-positive isolate displayed a considerably larger quantity of mucus compared to the second string positive isolate M20, and the other isolates tested. Two out of three K64 and K51 isolates were comparable in terms of mucus production, but one isolate from each group (M48 and M50) had relatively lower mucus production. Interestingly, only the isolate M48 tested positive for *rmpA2* gene, but this sample also showed a frameshift change. This mutation might perhaps explain the reduced production of mucus. However, the M17B isolate had the lowest mucus production, and notably, it belonged to the K2-serotype. There are also few observations, that have shown that there are differences in the thickness of mucus within the same capsular type of *K. pneumoniae* bacteria, suggesting that there is a complicated interaction of genetic variables that affect this

characteristic. Research has shown that the occurrence of hmv and non-hmv subpopulations within the same group of genetically identical organisms may be influenced by mutations and genes associated with transportation and central metabolism (Liang et al., 2024). Moreover, the existence of hypermucoviscous regulators and the absence of typical capsule regulators in some strains emphasize the need for additional research on the epidemiological significance of these differences in mucoviscosity among the identical capsular type of *K. pneumoniae* (Altayb et al., 2022). The level of hypermucoviscosity might differ among *K. pneumoniae* strains of the same capsular type, with a predominance of hmvKp isolates attributed to capsular type K2 (Osama et al., 2023). The variation in mucoviscosity within string-positive *K. pneumoniae* isolates may be explained by variables such as the presence of distinct virulence genes and antibiotic resistance profiles, as shown by numerous results (Osama et al., 2023). Moreover, the examination of the genetic composition of hmvKp isolates has shown that the hypermucoviscosity trait is frequently carried on plasmids and linked to particular virulence factors such as *rmpAC* and genes related to iron acquisition. These factors could potentially explain the variations in mucoviscosity observed in string positive *K. pneumoniae* isolates (M. Jin et al., 2023). Remarkably, none of our isolates tested positive for the *rmpAC* genes except M48 with a frameshift mutation in *rmpA2* gene. This implies that there might be a limited number of new genetic factors that contribute to the hypermucoviscosity phenotype. A similar observation was made by (Dey et al., 2022). in their investigation, where some isolates, such as P34, exhibited hypermucoviscosity even in the absence of these genes.

In the phagocytosis via neutrophils and serum killing experiment from this research, the isolate DJ (with the smallest capsule size) and the isolate M20 (with a positive string test) exhibited the least vulnerability to being engulfed by neutrophils. However, both isolates were vulnerable to serum-induced mortality, with one experiencing grade 3 severity and the other grade 2 severity. similarly observed an identical pattern, demonstrating that the assessment of virulence by neutrophil phagocytosis revealed *K. pneumoniae* isolates to have a relatively high resistance to phagocytosis, but were susceptible to serum death (Abate et al., 2012). We observed a link where the isolates DJ, M48, M50, and M20, which were the least sensitive to phagocytosis, had a somewhat bigger capsule size compared to the other isolates, except for DJ. Interestingly, all of them belonged to isolates that produce less mucus. The isolates with smaller capsule size, such as M17B, M57, and M58, exhibited greater sensitivity to phagocytosis. However, there was ambiguity about the mucoviscosity among these three isolates. It was shown that M17B and M57 were much less proficient in producing mucus compared to the isolate M58. Research

done by (L. Wang et al., 2017) revealed that serotype K1 and K2 strains, as well as ST11 isolates, had comparable profiles of virulence genes. However, the ST11 isolates shown had reduced levels of resistance to serum and phagocytosis compared to the serotype K1/K2 isolates. Surprisingly in our findings both the isolate M58, which is a generator of hyper mucus belonged to ST11, and the isolate M17B belonging to the K2-serotype, substantial phagocytosis was still observed, also they were susceptible towards serum mediated killing. As per the literature, while K1 and K2 capsular serotypes are often found in highly virulent strains of *K. pneumoniae*, there have also been instances of non-K1/K2 strains being detected among hypervirulent *K. pneumoniae* isolates. Additionally, it is important to note that not all K1 and K2 strains exhibit a hypervirulent phenotype (J.-C. Lin et al., 2014; Qu et al., 2015; I. R. Lee et al., 2016).

Furthermore, differences in susceptibility to phagocytosis were seen within the isolates of K64 and K51 serotypes. The isolate DJ, which belonged to the K64 type, showed the least susceptibility to phagocytosis. On the other hand, the isolate M51, which belonged to the K51 type, was shown to be the most sensitive to phagocytosis. Our investigation also revealed that isolate M58 which belonged to ST11 had a high mucus content and tested positive for the string phenotype. Remarkably, it exhibited a high susceptibility to human blood serum and was very vulnerable to phagocytosis. Recent research conducted in Rajasthan, India also shown comparable findings for an isolate exhibiting a string positive phenotype, hypermucoviscous colony, and reduced capsule formation. Additionally, this isolate was found to be sensitive to human blood serum (Dey et al., 2022). However, another string positive isolate M20, did not exhibit resistance against serum, interestingly even it was the second least susceptible to phagocytosis by neutrophils. Another intriguing discovery in our findings was that the M17B isolate, which belongs to the K2 serotype renowned for its highly virulent characteristics, did not exhibit any symptoms of hypervirulence in our investigation. The string phenotype was absent, there was a reduced amount of mucus, susceptibility to serum killing was seen, and vulnerability to phagocytosis was also noted.

The presence of ambiguity was observed about the minuscule dimensions of the capsule, the generation of mucus, serum-induced lethality, and phagocytosis. There are also few studies showed the differences among these phenotypic characteristics, of which a study from China documented significant variations in the serum killing pattern across different strains (ST412, ST218, ST592, ST268, and ST11) and K-types (D. Wei et al., 2021). However, their investigation did not uncover any significant association between Hypermucoviscosity, serum

killing, phagocytosis, and ST and K-type. Some researchers argue that MLST might be a suitable approach for identifying hvKp strains, instead of relying on string-phenotype and serum killing tests. This is because the virulence level of these isolates fluctuated during the investigation (Shi et al., 2018).

Curiously, in our study all the O2a isolates, regardless of their K-type or St type, exhibited either susceptibility or intermediate susceptibility to serum killing. Interestingly, all the O2a isolates, independent of their K-type or St type, showed either susceptibility or intermediate susceptibility to serum killing (grade 1 to grade 3), and were mostly susceptible in the phagocytosis experiment, except for isolate DJ. However, the isolates, on the contrary, belonged to the O1 serotype (M50 and M51) and mostly exhibited the serum resistance phenotype. (Sahly et al., 2004) also reported a similar discovery, where the O1 serotype was more often found in serum-resistant strains of *Klebsiella* groups, independent of their capacity to generate ESBLs, compared to serum-sensitive strains. Also, in a separate study conducted by (P. Hsieh et al., 2008), it was shown that out of the nine non-tissue-invasive strains of *K. pneumoniae* clinical isolates, eight strains belonging to the O1 serotype were resistant to serum-induced death. In contrast, the O2a was mostly associated with serum-sensitive isolates detected in our study. In addition, half of the O1 isolates (M48 and M50) exhibited reduced susceptibility against phagocytosis. Three (M48, M50, and M51) out of four isolates from this O1 group exhibited serum resistance at the grade 4 to grade 6 level. And the M50 (O1 + K51) isolate was the only one that exhibited both grade 6 serum resistance and a reduced sensitivity to phagocytosis, while the isolate M48 (O1 + K64) demonstrated grade 4 serum resistance and showed reduced susceptibility to phagocytosis. Based on this the primary data, it can be inferred that the virulence of *K. pneumoniae* isolates is attributed to O-type, regardless of K-type. The serotype O1 was identified as the primary virulence challenge among *K. pneumoniae* isolates from India. Furthermore, it is worth noting that there is a correlation between serum resistance and the presence of the O1 serotype. This suggests that the higher occurrence of the O1 serotype in multidrug-resistant strains, along with their greater resistance to the bactericidal effects of serum, may indicate a higher level of pathogenicity in drug-resistant strains compared to susceptible strains (P.-F. Hsieh et al., 2012; Fang et al., 2016b).

Research on *K. pneumoniae* strains has shown diverse associations between O and K antigen types and their effects on serum killing and phagocytosis. While some strains demonstrate a connection between antigen types and pathogenicity, others do not. For example, serotype K1 bacteria that had alterations in their O-antigens were able to avoid being engulfed by

neutrophils (Yeh et al., 2007, 2016), Whereas K7-type *Klebsiella* did not exhibit a notable association between capsule type and resistance to serum or elimination by phagocytosis (Podschun & Ullmann, 1998). Moreover, there have been findings suggesting that the existence of certain virulence-associated genes, such as *rmpA* and aerobactin, in specific hypervirulent isolates, has contributed to their ability to withstand phagocytosis and serum killing (Siu et al., 2012). The correlation between the mucoid phenotype, serum bactericidal activity, and phagocytosis in *K. pneumoniae* is intricate and influenced by multiple factors. Although certain studies indicate a connection between the mucoid appearance and the rates of phagocytosis, there is no clear link between the mucoid phenotype and resistance to serum or phagocytosis (Podschun & Ullmann, 1998; Cavalcanti et al., 2019). An earlier study showed that sequence types did not correspond with the ability of *K. pneumoniae* strains to escape phagocytosis or be devastated by serum, suggesting that strain phenotype and these immune responses are not directly related. However, later in different study by (Chiang et al., 2016), demonstrated an association between MLST and serum lethality in *K. pneumoniae*. Their investigation revealed that ST11 strains are resistant to serum, whereas ST258 strains are vulnerable to serum. This finding has implications for the pathogenicity of these strains (Siu et al., 2012). According to a recent study, the author discovered that genetic changes could cause variations in serum resistance and phagocytosis within the same O-serotype of *K. pneumoniae*. These variations have an impact on bacterial persistence and interactions with the host (Bain et al., 2023). Apart from this, variation in serum killing profile and phagocytosis within the same O-serotype has also been noted in many studies (Sahly et al., 2004; Yeh et al., 2016; Kuo et al., 2019; Short et al., 2020).

Research conducted on *K. pneumoniae,* and *E. coli* strains has revealed that the relationship between K-type, O-serotype, and serum sensitivity and phagocytosis is intricate and differs among various bacterial strains (Devine & Roberts, 1994; Lepper et al., 2003; Yeh et al., 2016). Although both K and O antigens are required to protect against phagocytosis and complement-mediated serum death, the precise interactions vary depending on the strain's properties.

Overall, many papers indicate that there is little correlation between hypermucus phenotype, string positive, ST and K-type with phagocytosis and serum killing, while many other reports indicate that there is no correlation between the two; our data support these observations. Therefore, our study merits confirmation using a larger number of isolates and considering all variables, including string positivity, hypermucoviscosity, K-type, O-type, and STs. In this study, all isolates were found to be positive in the qualitative detection of siderophore.

However, discrepancies were noted in the quantitative assessment of siderophore. Nevertheless, although there were variations in the quantitative ability of siderophore production in *K. pneumoniae*, the isolates belonging to XDR and PDR had a higher amount of siderophore compared to the MDR and Susceptible isolates. However, several XDR isolates (namely M6, M56, and ST1) exhibited reduced siderophore synthesis. Few XDR isolates such as M53 and M57 exhibited siderophore production percentages exceeding 20%. Like our findings, several investigations have shown that XDR and PDR isolates of *E. coli* and *Proteus mirabilis* exhibited higher amounts of siderophore synthesis compared to MDR and susceptible strains (Algammal et al., 2021; Khazaal et al., 2022). This suggests a possible association between siderophore production and antibiotic resistance. In order to investigate the impact of Iron and DIP (Iron chelator) on the growth and siderophore production of specific isolates (M10, M33, M48, M50, M51, and M52), it was observed that none of the isolates produced siderophore when exposed to iron. Similar, several studies have also demonstrated that high levels of iron restrict the formation of siderophores, and vice versa (Russo et al., 2011; Holden et al., 2018; T. Chen et al., 2020). However, the growth of all isolates was enhanced, regardless of their drug resistance and genetic profile associated with siderophore. While the presence of DIP had an impact on its growth, all isolates, regardless of their drug resistance profile, exhibited a notable decrease in growth. In accordance with our study, few researchers have demonstrated the potential efficacy of DIP as an antibacterial agent against prevalent nosocomial infections (Thompson et al., 2012). The metal chelator DIP, which binds to iron, was applied at various concentrations as stated above. The purpose of adding DIP was to chelate even small amounts of iron in the media. By using DIP in the media solution, we can replicate the natural conditions found in the body, where iron is chelated by proteins like lactoferrin and transferrin (Bachman et al., 2012). Thus far, the combined usage of deferasirox with vancomycin has demonstrated promising effects against MRSA (G. Luo et al., 2014). Similarly, the combination of doxycycline and the CP762 (iron chelator) has shown potential against *P. aeruginosa* (Faure et al., 2021). Furthermore, the triple combination of deferasirox, thiostrepton, and doxycycline, has exhibited promising effects against both *P. aeruginosa* and *A. baumannii* in both laboratory tests and animal models (Chan et al., 2020). Iron chelators can be beneficial in treating microbial diseases by reducing the amount of iron available, thereby preventing the generation of reactive oxygen species (ROS), and by suppressing microbial growth through nutritional deprivation (C. Lehmann et al., 2021; Paterson et al., 2022). Nevertheless, there was ambiguity noted in the percentage of siderophore formation. All the isolates exhibited either equivalent or greater levels of siderophore synthesis

when exposed to a concentration of 400 uM of DIP. Researchers reported similar findings, demonstrating that the addition of 2,2'-dipyridyl (DIP) greatly enhances the synthesis of siderophores in *Klebsiella* species. Studies have demonstrated that depriving *K. pneumoniae* of iron in the culture medium through DIP significantly increases the production of siderophores (Sah et al., 2015). Meanwhile, other concentrations (200 uM, and 100 uM) exhibited either a higher or lower amount of siderophore among the tested isolates. Remarkably, isolate M48 had the highest siderophore synthesis, reaching over 30%, when DIP was added. This isolate possessed all the genes associated with aerobactin and yersiniabactin, whereas its siderophore production without DIP was only around 5%. However, other isolates of M50 with similar characteristics exhibited a lower level of siderophore synthesis, approximately 6% and 3% with DIP and without DIP, respectively. Unexpectedly, the M10 isolate, lacking aerobactin and yersiniabactin genes, exhibited a significant increase in siderophore production, going from less than 5% to over 20%, upon the introduction of DIP.

Regarding antibiotics, all examined isolates exhibited either equivalent (M48, M50, M51, and M52) or slightly diminished growth (M10, and M33) in accordance with escalating concentrations of ampicillin. In relation to siderophore production, all of the isolates exhibited either no production of siderophores or lower production compared to the control, with the exception of M50, which showed more siderophore production than the control at a concentration of 40 ug/ml of ampicillin. This suggests that *K. pneumoniae*, due to its synthesis of beta-lactamase, does not need extra factors like siderophore formation to withstand beta-lactam antibiotics (such as Ampicillin) (Kirienko et al., 2013). The presence of ciprofloxacin resulted in a notable decrease in growth when larger concentrations of the antibiotic (5 ug/ml and 10 ug/ml) were introduced, demonstrating a considerable reduction in growth in isolate M10. However, a decrease was also detected in M33, but it was not statistically significant. While all other isolates were rather stable in terms of growth in the presence of ciprofloxacin. Notably, all the isolates, regardless of their genetic makeup, exhibited a substantial rise in siderophore synthesis. This increase was greater than that observed in the control of each isolate, and it corresponded with higher concentrations of ciprofloxacin. A further noteworthy finding was that all isolates demonstrated a minimum of about 20% siderophore production when exposed to 10 ug/ml of ciprofloxacin. And strain M33 exhibited siderophore synthesis of approximately 50% at a ciprofloxacin concentration of 10 ug/ml. Currently, there is no documented direct relationship between elevated siderophore production and heightened antibiotic resistance. Literature studies have shown that siderophore synthesis indirectly

benefits bacteria by lowering oxidative stress, hence increasing antibiotic resistance. This occurs when siderophores are synthesized intracellularly and then attach to deleterious radical ions, facilitating their extracellular transit. As a result, oxidative stress is diminished, ultimately resulting in heightened antibiotic resistance (Y. Zhang et al., 2016). All isolates, except for M48 and M50, exhibited a decrease in growth due to colistin. However, the drop was statistically significant in all isolates except in M51. The presence of ambiguity was observed in siderophore formation. Approximately 50% of the tested isolates did not exhibit siderophore synthesis at most of the concentrations of colistin. Conversely, the remaining isolates demonstrated a reduction in siderophore production as the concentrations of colistin increased, with the exception of the PDR isolate M50.

Overall, when the isolate is resistant to ampicillin and is treated with ampicillin, it can potentially enhance the growth of resistant isolates, as observed with PDR isolate M50. However, it is surprising that this treatment can also reduce the virulence properties of the isolates, such as suppressing or reducing siderophore production. While the isolates resistant to ciprofloxacin could lead to increased severity in patients when treated with greater doses of ciprofloxacin, our findings indicate that all isolates showed significantly higher levels of siderophore production when exposed to ciprofloxacin. Nevertheless, colistin remains a preferred therapeutic option due to its ability to inhibit bacterial growth and either suppress siderophore synthesis or reduce it. However, it can also be challenging in the case of PDR isolates or isolates resistant to colistin, as demonstrated in our research. We found that a PDR isolate called M50 exhibited no growth when exposed to colistin, but we noticed an increase in the percentage of siderophore when exposed to colistin doses above the minimum inhibitory concentration, at the MIC, and even at below MIC levels.